

# UNIQUE NANO PHENOMENA

## Introduction

- “***Intensive properties***” such as the *color, melting point, electrical conductivity, magnetism, ionization potential, electron affinity, etc.* which do ***not*** depend on the ***size or volume*** become size-dependent (***extensive properties***) for the **nanomaterials**.
- *Unique properties of nanomaterials arise mainly* from their **small sizes** leading to the
  - (i) **quantum confinement effects** and
  - (ii) **large surface area to volume ratio.**
- At the **nanoscale**, ***the structure, size, morphology, and proximity of the nanomaterials affect their quantum confinement and surface-interface effects*** which give rise to the ***novel physical and chemical properties*** in the nanomaterials.

❑ *At what size do the quantum size effects begin to appear?*

- **(i) Quantum Effects ( $D \sim$  or  $< l$ ):** According to Gleiter's definition, when the **characteristic size** ( $D$ ) (viz., *diameter, thickness, length*) of the *building blocks* of microstructures becomes comparable to or less than the **length scale** ( $l$ ) of the **physical phenomenon** (viz., *mean free path length of electrons, phonons, etc.; coherent length, screening length*), the *quantum size effects on the material properties begin to appear*.
- The *length scale* ( $l$ ) of most of the physical phenomena lies in the *nanometer scale* (e.g., the **Bohr radius of an electron in silicon is ~4 nm**), the *confinement* of electrons, phonons, and photons occurs and therefore the **quantum effects** play important roles in determining the properties of the materials. Therefore, the *nanomaterials show size- or shape-dependent properties*. Many properties of materials such as *optical, magnetic, electric, etc. drastically change* from that traditionally observed for *bulk materials*.

❑ Why are **SURFACE-INTERFACE EFFECTS** significant in nanomaterials?

➤ (ii) **Surface Effects:**

➤ (ii.A) The ***fraction of the surface atoms becomes significant*** with respect to the total number of atoms in the nanomaterials (due to their ***large surface area-to-volume (A/V) ratio***).

➤ The large fraction of the surface atoms leads to various effects.....

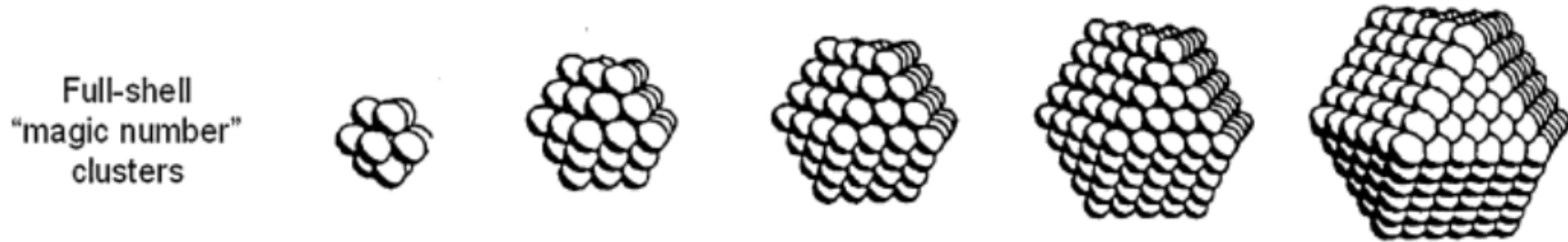
✓ Properties such as ***surface adsorption, melting point, solubility, chemical reactivity, etc. are affected by the large surface area to volume ratio of the nanomaterials. The surface-interface effects also play very significant roles*** in the properties of the nanomaterials.

✓ For example, ***nonmagnetic gold becomes magnetic*** in the form of nanoclusters due to the ***enhancement of the magnetic moments on the low coordinated atoms at the surface.***

## ❖ *Calculation of Fraction of Atoms at the Surface*

- ❑ Let us calculate the **percentage of surface atoms in close-packed (hcp) full-shell clusters** of different sizes.
- Full-shell clusters are built up by hexagonal (hcp) or cubic (ccp) close-packed atoms, *as is the case in most bulk metals*, consisting of a central atom that is surrounded by 1, 2, 3, . . . ,  $n$ , . . . dense-packed *shells*.
- ✓ The **total number of atoms**  $= 1 + \sum (10n^2 + 2)$ , where  $n = 1, 2, 3, \dots$ , number of shells in the cluster.
- The smallest *full-shell* cluster ( $n = 1$ ) consists of  $1 + 12 = 13$ , the next ( $n = 2$ ) of  $13 + 42 = 55$  atoms, and so on.
- The *number of atoms per shell* (in the  $n$ -th shell) is given by  **$(10n^2 + 2)$** .

# Close-Packed Magic Number Clusters




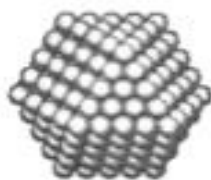
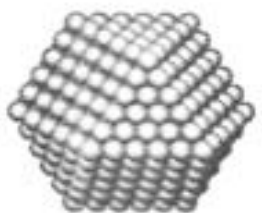
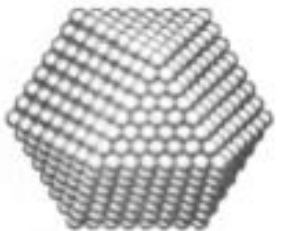


$n =$	Number of shells	1	2	3	4	5
$1 + \sum(10n^2 + 2) =$	Number of atoms in cluster	13	55	147	309	561
	Percentage of surface atoms	92	76	63	52	45

- Magic Number = Cluster has a complete, regular outer geometry
- Formed by successively packing layers around a single metal atom.
- Number of atoms ( $y$ ) in shell ( $n$ ):  $y = 10n^2 + 2$  ( $n = 1, 2, 3, \dots$ )
- Maximum number of nearest neighbors (metal-metal hcp packing)
- Decreasing percentage of surface atoms as cluster grows

**Table 2.1** contains some information on the percentage of surface atoms in close-packed full-shell clusters of different sizes.

- *Number of atoms per shell* is given by  $(10n^2+ 2)$ , and
- **Total number of atoms** =  $1+ \sum(10n^2+ 2)$ , where  $n = 1, 2, 3, \dots$ , number of shells in the cluster.
- **Fraction of surface atoms** =  $(10n^2+ 2)/[1+ \sum(10n^2+ 2)]$

TABLE 2.1 The relation between the total number of atoms in full shell clusters and the percentage of surface atoms			
Full-shell Clusters		Total Number of Atoms	Surface Atoms (%)
1 Shell		13	92
2 Shells		55	76
3 Shells		147	63
4 Shells		309	52
5 Shells		561	45
7 Shells		1415	35



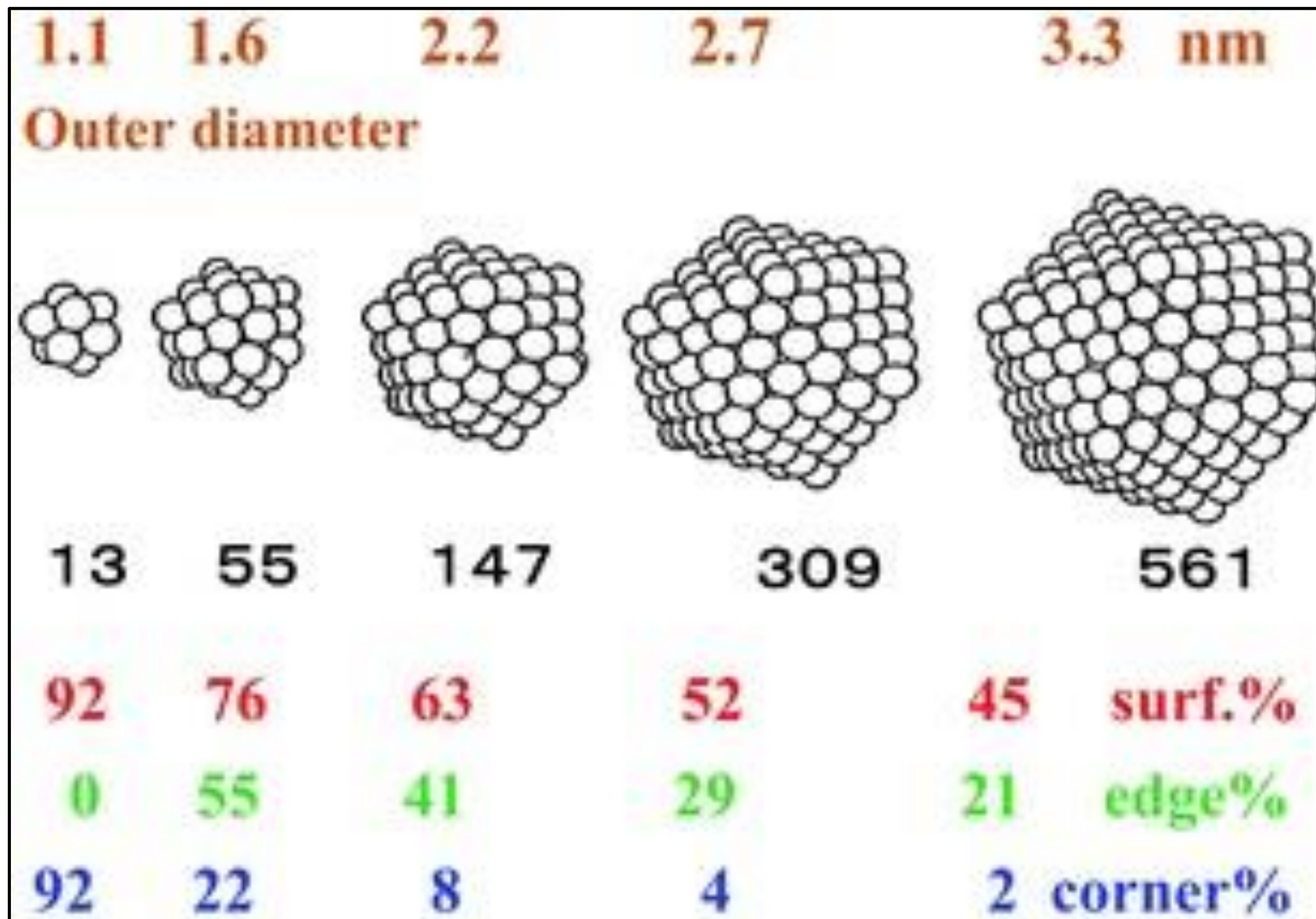
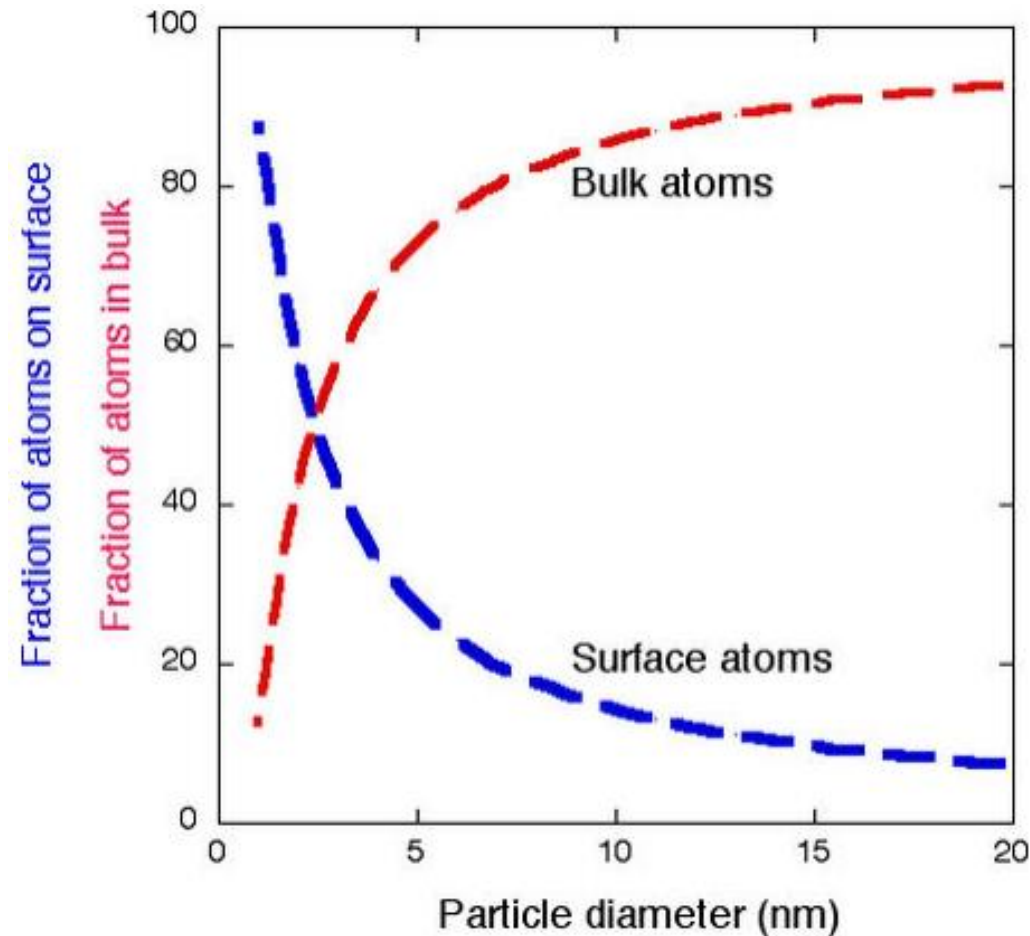


Fig.....Magic numbers of Au nanoparticles and their sizes.

❖ The surface of a **sphere** scales with the square of its radius  $r$ , but its volume scales with  $r^3$ .

➤ The **total number of atoms**  $N$  in this sphere *scales linearly with volume*.

➤ The *fraction  $F$  of atoms at the surface is called **dispersion**, and it scales with the surface area divided by volume*, that is, *with the inverse radius*, and thus with  $N^{-1/3}$ .

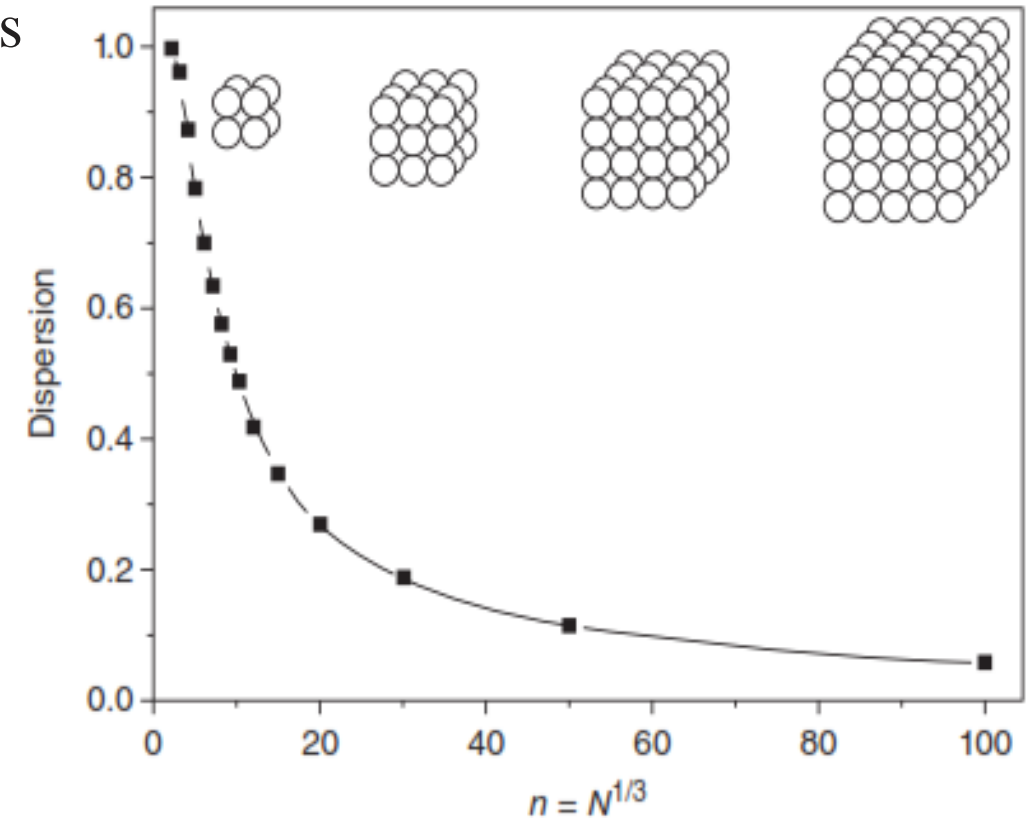




❖ The dispersion,  $F$ , of the **cubic crystal** with a total of  $N$  atoms  $\approx \frac{6}{N^{\frac{1}{3}}}$ .

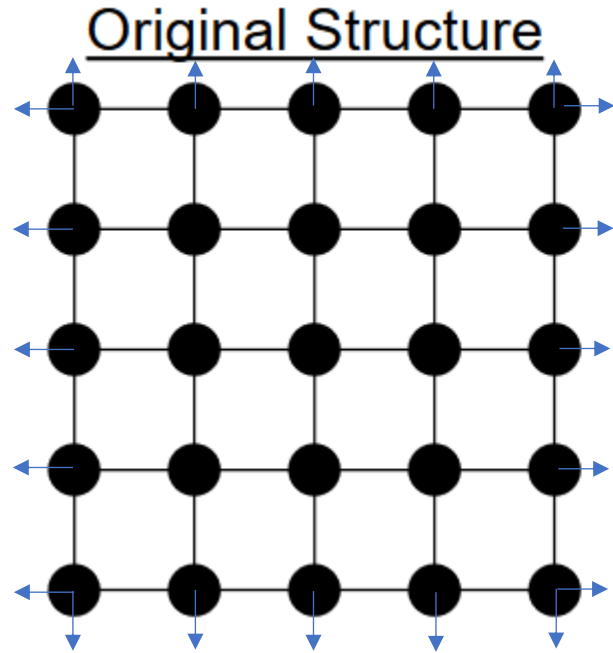
- The **dispersion**,  $F$ , is illustrated in Figure 8.5 for the **cubic crystal** with  $n$  atoms along an edge and a total of  $n^3 = N$  atoms.
- *The structure of the first four clusters is displayed.*
- The atoms are counted, and  $F$  is calculated as follows

$$F = \frac{6n^2 - 12n + 8}{n^3} = \frac{6}{N^{1/3}} \left( 1 - \frac{2}{N^{1/3}} + \frac{8}{6N^{2/3}} \right) \approx \frac{6}{N^{1/3}}$$



**Figure 8.5** Size dependence of the dispersion for cubic particles with  $n = N^{1/3}$  atoms along an edge.  
© 2006. With permission of RSC.

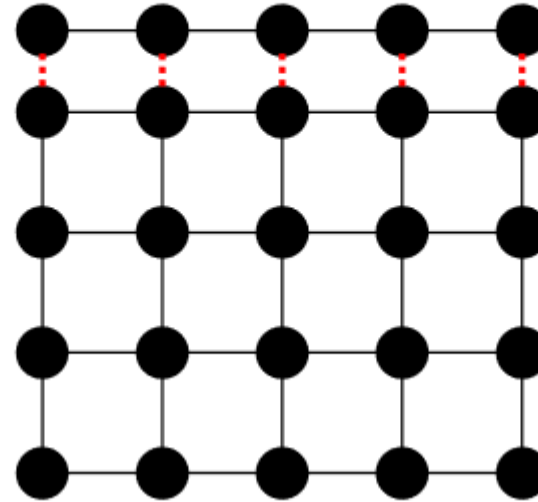
❖ The *surface atoms differ from the bulk atoms in many ways.*



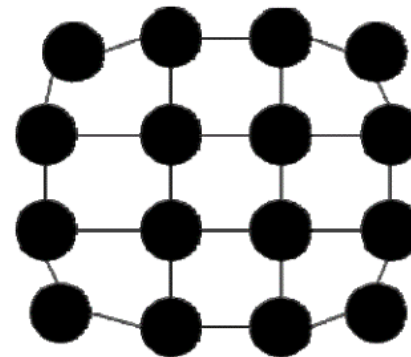
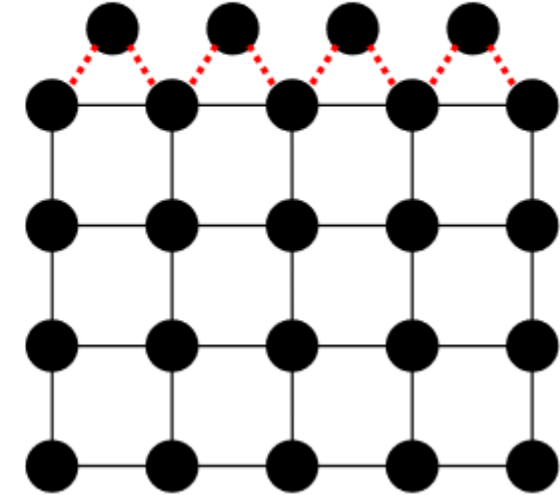
bulk crystal

(arrows show extended nature of the crystal)

Shortened Surface Bonds



Shifted Surface Bonds



**nanocrystal**

- **Strained bonds** of the surface atoms
- *Exchange or sharing of electrons greatly affects the lattice bonds*
- *Surface Reconstruction and relaxation*

➤ **For Nanomaterials Surface Matters a lot....**

❖ The *surface atoms differ from the bulk atoms in many ways.*

❑ ***Coordination Number:*** There are *properties that are not directly dependent on the electronic situation in the particles but are rather a consequence of the averaged coordination number of the participating atoms.*

➤ The *coordination number of a surface atom is smaller than that of a bulk atom.*

➤ C.N. of FCC (bulk) = 12.

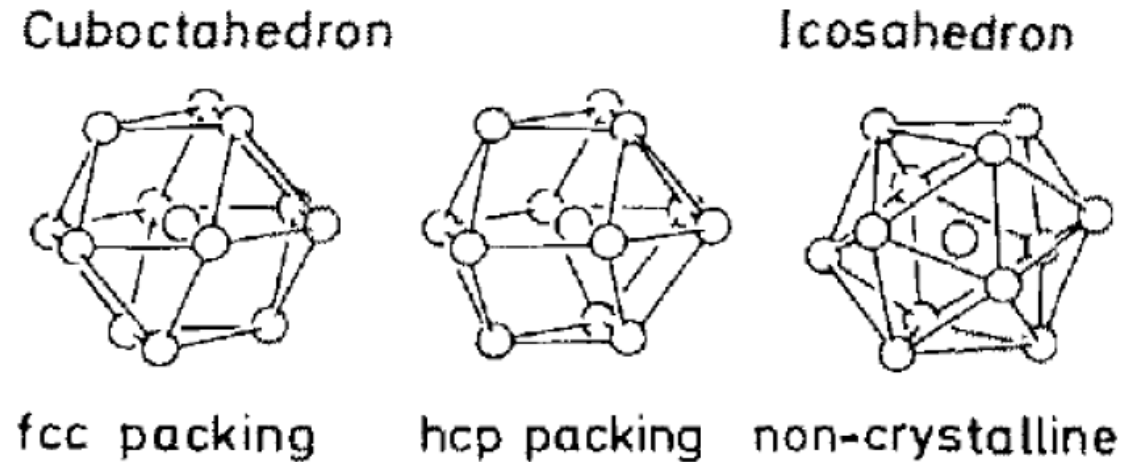
✓ For example, a gold atom in bulk face-centered cubic Au has 12 near neighbors, but a gold atom on the (111) surface of the crystal (the most dense crystal plane of gold) has *six nearest neighbors in-plane* and *three underneath*, for a total of 9.

➤ *Surface atoms have several unsaturated coordinations (under-coordinated) or dangling bonds.*

➤ *A surface atom has unsatisfied bonds which make it chemically very active.*

## Coordination Number

➤ By far the majority of metals form hexagonal or cubic close-packed structures with coordination numbers of 12, except for surface atoms when it is 9 or smaller, depending on whether faces, and which kind of faces, edges, or comers are considered.



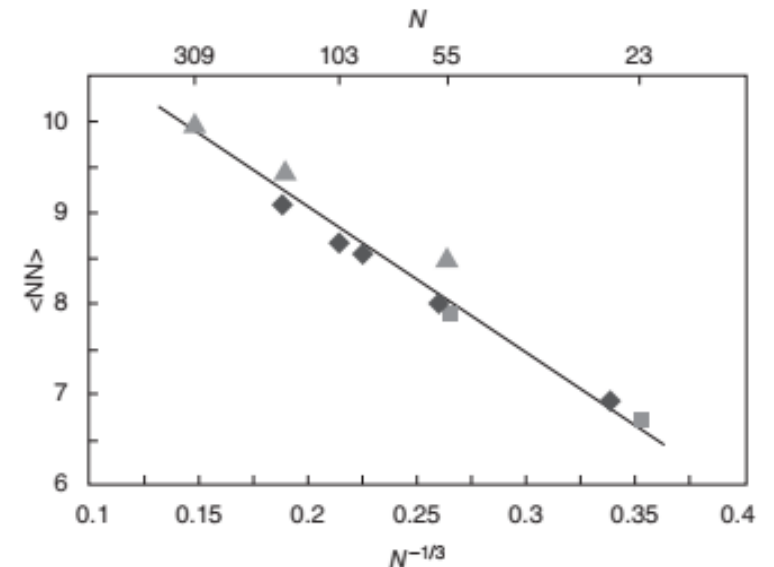
**Fig 2.** The model of close packings of rigid spheres: Face-centered cubic (fcc), hexagonal close packing (hcp) and the N=13 icosahedron.

- In fcc and hcp, the central atom is surrounded by 12 nearest neighbors.
- An icosahedron is more spherical.

- ❑ All *properties that depend on the dispersion* of a particle lead to a straight line when plotted against  $r^{-1}$ ,  $d^{-1}$ , or  $N^{-1/3}$ .
- **Atoms at the surface have fewer direct neighbors than atoms in the bulk.**
- Therefore, *particles with a large fraction of atoms at the surface have a low mean coordination number* (which is the number of nearest neighbors).
- In fact, the *dispersion and the mean coordination number*  $\langle NN \rangle$  *obey the same scaling law and are equivalent measures of surface effects*.
- The linearity of a plot of  $\langle NN \rangle$  against  $N^{-1/3}$  is shown in Figure 8.6 for small clusters of Mg atoms in various packing symmetries. *In the limit of infinitely large clusters, the line extrapolates to  $\langle NN \rangle = 12$ , the coordination number of close-packed spheres in the bulk.*

**Figure 8.6** Calculated mean coordination number as a function of inverse radius for magnesium clusters of different symmetries (*triangles: icosahedra, squares: decahedra, diamonds: hexagonal close packing*).

© 2001. With permission of RSC.





## ❑ *Surface relaxation* and *surface reconstruction*

➤ Because of a smaller *coordination number*, the *surface atoms experience an unbalanced force* which is relieved by a readjustment in their positions by “*surface relaxation*” and “*surface reconstruction*”.

❑ The *surfaces also have many types of defects*.

➤ Because of these factors, *in addition to the chemical activity, the other properties (electronic, magnetic, mechanical) of the surfaces may be quite different from those of the bulk.*

## ❖ For Nanomaterials Surface Matters....

- For **bulk materials**, the **number of surface atoms** w.r.t. to the total number of atoms is **negligible**.
- The *smaller a particle becomes, the more the proportion of surface atoms becomes*.
- Hence **the properties of material change when they are in the form of nanocrystals**.
- ✓ Among the several manifestations of the *dominance of the strained surface bonds include lower melting points* for nanomaterials.
- The *melting point (m.p.) of a solid is reached when the order of the lattice is beginning to be destroyed*. **For a distinct solid m.p. is a physical constant**, but only so long as the surface is negligibly small in comparison with the total volume—that is, **for typical bulk material**.
- ✓ A spherical particle of 50 nm in diameter has about 6% of surface atoms so for micrometer-sized or even millimeter-sized particles these atoms can indeed be neglected. If percentages are reached as given in Table 2.1, *the number of surface atoms becomes equal to or even exceeds the number of inner-core atoms*.

✓ As *the coordination number of surface atoms is 9 or smaller*, these atoms are more easily rearranged than those in the center of the particle: *the melting process starts earlier*. There is a dramatic decrease in melting points for particles smaller than 3 – 4 nm.

❖ The **dominance of surface atoms leads to a heightened chemical reactivity**. The *chemical activity of a material increases drastically as the particle size reaches a few nm*.

➤ A dramatic manifestation of this is the *auto-ignition* of fine metal powders in the air (e.g., the use of Al powder as rocket fuel). Aluminum metal in the form of a fine powder acts as fuel for rocket engines, including the booster stages that were used in space shuttle launches.

➤ Since the *dispersion of nanomaterials is high*, it is important to understand *surface effects and their implications in giving rise to the unique physical, chemical, and biological properties, which radically differ from their bulk counterparts* owing to the *presence of a large number of surface atoms*.

## ❖ Surface Matters.... for Nanomaterials

- The *surfaces* play a crucial role in such phenomena as the shape of the nanoclusters, synthesis of nanoparticles, catalysis, sintering, etc.
- Additionally, many of the important processes such as *nucleation, growth, dissolution and precipitation, chemical reactions, adsorption, surface modification, self-assembly*, etc. occur at the *interface between different phases* (solid, liquid, and gas).
- Synthesis, processing, self-assembly, and properties of nanoscale objects are therefore *very sensitive to parameters* such as *specific surface area, surface structure, surface curvature, and surface energy*.
- *These quantities play an increasingly dominant role as the size of an object decreases to below submicron levels.*
- In this section, we first discuss these surface properties and illustrate them with some examples of their application to nanostructures.

## ❑ Effects of Surface Energy Differences

❖ Various properties change with this surface energy

➤ The melting point of nanoparticles can be hundreds of degrees below that of the bulk material

➤ Additionally, nanoparticles have lower boiling points, higher vapor pressures, higher solubility, and higher reactivities

➤ Here we will apply some **classical thermodynamics concepts** to some general properties of *nanoscale systems*, and in particular begin *to understand what the effect of the size of a particle* is on particular system properties.

## ❖ *Increased Surface Energy and Tension*

- Having *the large surface*, the nanocrystals have therefore *extended external free surface energy* (Gibbs energy) and given by the Equation:

$$dG = -SdT + VdP + \sum_i \mu_i dn_i + \gamma dA$$

where  $T$  is the temperature of the system,  $S$  the entropy,  $P$  the pressure,  $V$  the volume,  $\mu_i$  the chemical potential of species  $i$ ,  $n_i$  the number of moles of species  $i$  in the system,  $\gamma$  the interfacial energy, and  $A$  the interfacial area.

- $\gamma$  is a specific surface energy (the energy per surface unit), or a specific work to create the free surface area,  $dA$ , or a specific tension. Therefore, we can write:  $\gamma = \left( \frac{\partial G}{\partial A} \right)_{T,p,n_i}$
- The above equation says that  $\gamma$  is *the work necessary to reversibly extend the interface by unit area at a constant temperature, pressure, and composition of the system*, redefining  $\gamma$  with respect to parameters that are definitively more familiar and more accessible to measurements as well.



- $\gamma$  has the dimensions of energy per unit area ( $\text{J/m}^2$ ) that can be alternatively written as force per unit length ( $\text{N/m}$ ), which justifies the possibility of both energetic and mechanical definition/interpretation of  $\gamma$ .
- ✓ For isobaric and isothermal transformations,  $G$  allows to “squeeze” the total change of the entropy of the system and its surroundings in terms of change of the system alone and to write:  
 $(\partial G)_{T,p} \leq 0$  which says that *any system spontaneously strives to reduce its Gibbs energy*.
- By merging the above two equations we can deduce the *thermodynamic fundament to the usual mechanistic explanation of  $\gamma$* .
- Note that by definition of an *intensive variable*,  $\gamma$  is **positive**; that is, it is assumed that an increase of  $A$  raises  $G$ .
- Actually,  $(dG)_{T,p,n} < 0$  implies  $dA < 0$ , and therefore, at constant  $T$ ,  $p$ , and  $n_i$ , *an interface spontaneously tends to contract*.

- The above relation is in agreement with the machinery that rules *molecular trade between two bulk phases separated by an interface*.
- In the *bulk phases* (on the condition they are isotropic), each molecule is equally attracted by its neighbors so that the *net force acting on that molecule averages to zero*.
- Instead, *at the interface*, the *molecules are in an asymmetrical force field, being attracted toward the phase with the strongest cohesive attraction force*. *As a result, the molecules tend to leave the interface, and thereby the interfacial area, to contract to its minimum—which is the reason why rain droplets are spherical and not cubic*.
- *On the other hand, this means that bringing molecules from the bulk to the interface needs an “extraction” work that the molecules in the interface gain in the form of higher potential energy*.
- Finally, it is important to note that from this machinery, it follows that *the interfacial tension increases as the difference between the cohesion forces within the two adjoining bulk phases increases*.

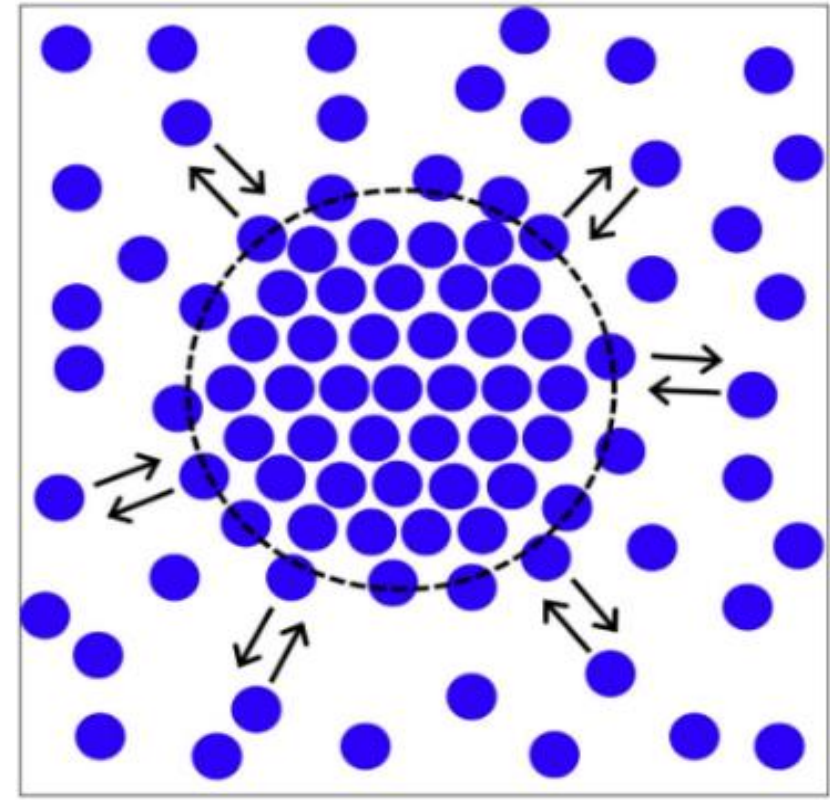
# ❑ Size Dependence of **Melting Temperature** and **Solubility** of Nanoparticles

- We will present in the following a highly simplified argument that avoiding grinding through heavy mathematics will (try to) deliver the essence of the subject. Both the treatments are based on the criteria of equilibrium for systems that are made of a bulk solid phase and a bulk liquid phase separated by a curved solid-liquid interface.
- ❖ **Criteria for Solid-Liquid Equilibrium:** *For a spherical particle, the **particle molar Gibbs energy is given** by the **(bulk interior + surface)** contributions.*
- When a system is *in equilibrium*, its overall state does not change in time. Indeed, fluctuations occur on atomic and/or molecular level, but they are random, and therefore, there is not a net flux of transformation at the macroscopic scale. Such a state can be formally described by saying that *the macroscopic properties of the system do not change*. In particular, for the Gibbs energy, at isothermal and isobaric conditions it has the following form:

$$(dG)_{T,p} = \sum_i \mu_i dn_i + \gamma dA = 0$$

- Now, *consider a system made of spherical particles* of a *pure* molecular (or atomic) substance.
- At the **melting temperature,  $T_m$** , the system is characterized by the *equilibrium between the solid particles (the solid phase) and the surrounding liquid from the melted particles* (the liquid phase).
- **At the microscopic scale**, this means the **number of atoms or molecules ( $dn_s$ ) per unit time that escape from the solid phase into the liquid phase** by crossing the solid-liquid interface equals the number of atoms or molecules ( $dn_L$ ) that perform the opposite trip (Figure 1.2).

**FIGURE 1.2** Microscopic scale cartoon of the equilibrium between a solid particle (bulk solid phase) and the surrounding liquid from melted particles (bulk liquid phase). The solid-liquid interface is evidenced by the black dotted line.



- The *infinitesimal change in Gibbs energy* for such a system can be written by adapting the following fundamental Equation at constant  $T$  (i.e., at  $T_m$ ) and  $p$  and reads

$$(\partial G)_{T,p} = \mu_L dn_L - (\mu_S dn_S + \gamma_{SL} dA_{SL})$$

where the subscripts  $S$  and  $L$  refer to the solid and liquid bulk phases, respectively, and the subscript  $SL$  refers to the solid-liquid interface.

- At equilibrium,  $(\partial G)_{T,p} = 0$  and  $dn_L = dn_S = dn$ , and the above Equation rearranges into

$$\mu_L = \mu_S + \gamma_{SL} \frac{dA_{SL}}{dn}$$

- If instead of  $dn$  we write  $dm$  (small *mass* change), then:

$$(\partial G)_{T,p} = \mu_L dm - (\mu_S dm + \gamma_{SL} dA_{SL})$$

- In our case, the solid phase is a spherical particle of radius  $r$  and molar density  $\rho$ ; therefore,  $dA_{SL} = d(4\pi r^2)$  and  $dm = d(\rho \cdot \frac{4}{3}\pi r^3)$  and finally the equation simplifies into:

$$\mu_L = \mu_S + \frac{2\gamma_{SL}}{\rho r} = \mu_P$$

The above Equation expresses the *critierion for equilibrium between the solid and the melted particle phases*.

- The right-hand side of the equation represents *the **molar** Gibbs energy of the whole particle,  $\mu_P$ , which is given by the sum of the chemical potential of the particle **bulk  $\mu_S$**  and of a term that accounts for **the molar surface energy contribution**. This term results linearly dependent to the **inverse of the particle radius  $r$** , viz., to the interface **curvature  $1/r$** .*
- *It is significant for nanoparticles where  $1/r \gg 0$ .*
- *It decreases as the size of the particle increases, and finally vanishes for infinite flat surfaces ( $1/r = 0$  or  $dA_{SL} = 0$ ) or, more generally, for bulk solids in which the surface energy contribution is negligible. (For bulk solid, the equilibrium criteria reduce to the familiar  $\mu_L = \mu_S$ .)*



- The surface energy causes the surface tension or the surface tangential force,  $F = \gamma a$ . The tension exists for any surface, including a plane surface.
- For nanoparticles of radii ( $r$ ), an additional Laplace tension ( $P_L$ ) is arisen which is given by Equation 8.4:

$$P_L = 2\gamma/r \quad (8.4)$$

- It is responsible for capillary phenomena and wetting of liquids.
- The Laplace tension for solid particles is often considered as Laplace pressure. For instance, for a small  $r = 10$  nm liquid nanoparticle, the Laplace pressure is very high (Eq. 8.5) and *is comparable with the pressure of gun powder gas in a gun barrel.*

$$P_L = \frac{2\gamma}{r} = \frac{\frac{2J}{m^2}}{10nm} = 200 \text{ MPa} \quad (8.5)$$

## *Melting Point Depression*

- **See the examples:** The m.p. of **bulk CdS** is 1675 K vs. m.p. of **CdS nanoparticle (diameter ~2.5 nm)** is 600 K; and m.p. of **bulk carbon 3800 K** vs. single wall carbon nanotube melts at **~1600 K**.
- We see *a decrease in m.p. at the nanoscale compared to the bulk matter*.
- The above **size-dependent chemical potential** argument can be used to describe the **melting temperature dependence on particle size**. In order to do this, we will need to analyze *the variation of the molar Gibbs energy (the chemical potential) with temperature*.
- Let us start by considering a mole of bulk phase (gaseous, liquid, or solid) made of the pure substance that constitutes the particle. The temperature dependence of the molar Gibbs energy is given by the partial derivative at constant  $p$ ,  $n$ , and  $A_{SL}$  of the fundamental Equation:

$$\left(\frac{\partial G_m}{\partial T}\right)_{p,n,A_{SL}} = -S_m$$

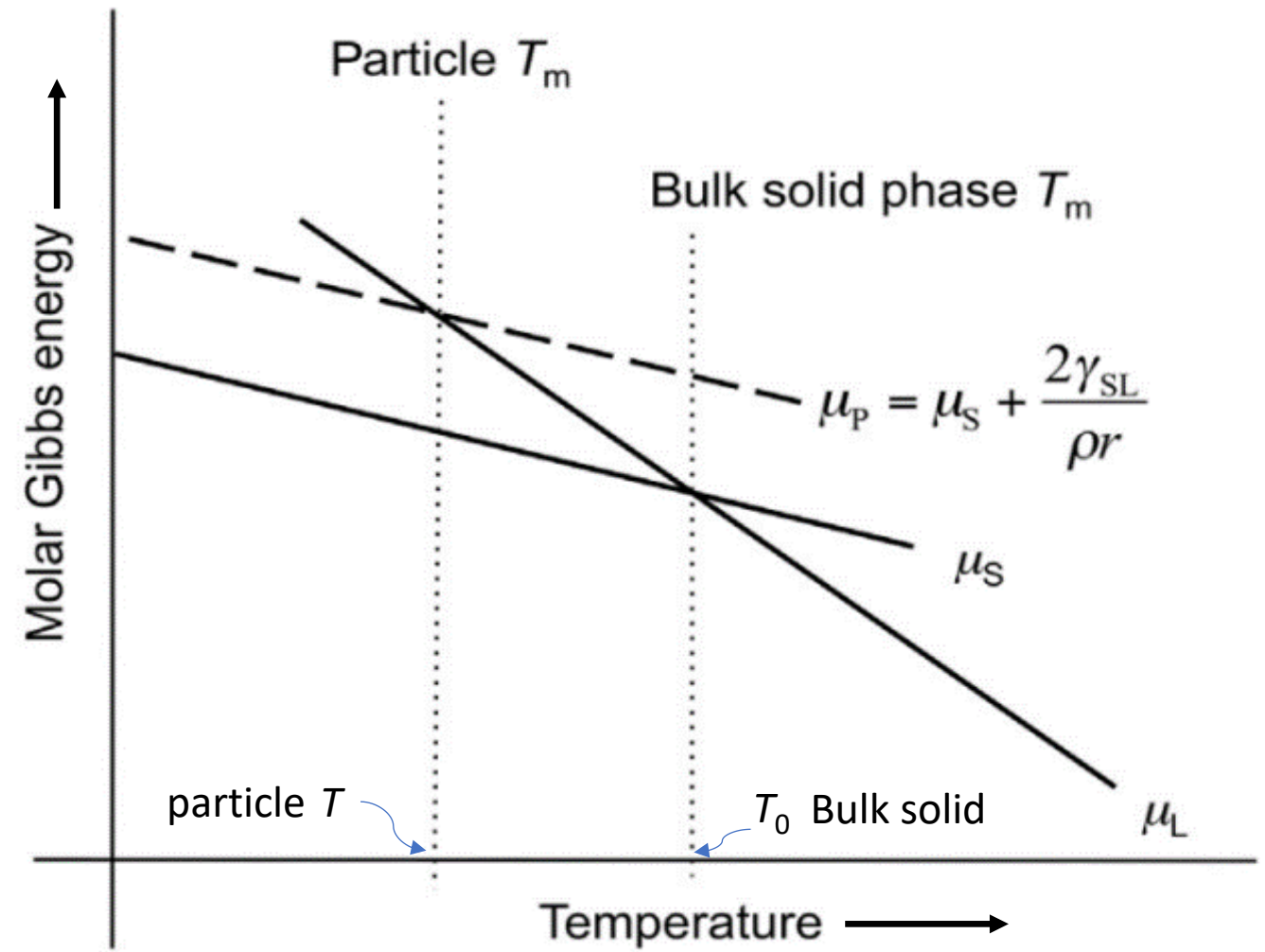
where the subscript  $m$  refers to the molar quantities.

- For *pure* substances, the *molar Gibbs energy coincides with the chemical potential* and the above equation can be rewritten as

$$\left(\frac{\partial \mu}{\partial T}\right)_{p,n,A_{SL}} = -S_m.$$

- This can be used to plot the variation of the chemical potential of the bulk solid phase,  $\mu_S$  and of the liquid phase  $\mu_L$ .
- They result in straight lines with the negative value of the *molar entropy*,  $S_m$ , as the angular coefficient or slope (Figure 1.3).
- As the  $S_m$  of the liquid phase is *greater* than that of the solid phase, the straight line representing the liquid phase falls more steeply with temperature than that representing the solid phase.

**FIGURE 1.3** Variation of the molar Gibbs energy with temperature at constant pressure and composition for a liquid phase ( $\mu_L$ ), a bulk solid phase ( $\mu_S$ ), and a spherical particle ( $\mu_P$ ). Note that the lines are straight in first approximation and actual lines are curved.



- The **melting temperature**,  $T_m$ , is given by **the intersection** of the solid- and liquid-phase lines that is ***the temperature at which the equilibrium criterion  $\mu_S = \mu_L$  is satisfied.***

- If we now consider a **spherical particle**, the particle overall molar Gibbs free energy (bulk *plus* surface) is given by

$$\mu_P = \mu_S + \frac{2\gamma_{SL}}{\rho r}$$

- Therefore, the variation of molar Gibbs free energy of the particle with temperature is a straight line parallel to the straight line of  $\mu_S$  **but raised by the factor**  $(\frac{2\gamma_{SL}}{\rho r})$ , which is proportional to the curvature  $1/r$ . This line is represented in Figure 1.3 by the dotted line.
- **Its intersection with the liquid-phase line ( $\mu_P = \mu_L$ ) locates the particle  $T_m$** , which results lower than the bulk solid phase  $T_m$ .
- *This effect is commonly referred to as **melting point depression** and becomes prominent for nanoparticles.*
- Finally, we may note that *the more the factor  $(\frac{2\gamma_{SL}}{\rho r})$  increases, the more the line intersection shifts to lower temperatures, suggesting a monotonic dependence of the melting point depression with the molar surface energy.*

- Melting point depression has been observed for free-standing, solid-supported, and matrix-embedded metallic and molecular nanoparticles, with *a decrease of  $T$  ranging from few to several tenths of percentage with respect to the solid bulk phase  $T_0$ .*

$$\frac{T - T_0}{T_0} = \frac{\Delta T}{T_0} = -\frac{2V_m(l)}{\Delta H_m} \cdot \frac{\gamma_{SL}}{r}$$

- First let us consider the **melting of a bulk** solid.

***Bulk Solid  $\rightleftharpoons$  Liquid***

$$\mu_S \overset{T_0}{\rightleftharpoons} \mu_L$$

- From the free energy balance at equilibrium (for a bulk system):

$$\Delta H \cdot dm - T_0 \Delta S \cdot dm = 0$$

Or

$$T_0 \Delta S = \Delta H. \quad \dots \dots \dots (1)$$



➤ Let us now consider the *melting of a small particle*. For the melting of a small particle:

***Small Particle Solid  $\rightleftharpoons$  Liquid***

$$\mu_P \overset{T}{\rightleftharpoons} \mu_L$$

$$\Delta H \cdot dm - T \Delta S \cdot dm - \gamma_{SL} \cdot dA = 0$$

Or

$$\Delta H - T \Delta S - \gamma_{SL} \frac{dA}{dm} = 0 \quad (\text{since } dm \neq 0) \dots\dots\dots(2)$$

➤ From eqns. (1) & (2),

$$T \Delta S - T_0 \Delta S = - \gamma_{SL} \frac{dA}{dm}$$

$$\Rightarrow T - T_0 = - \frac{\gamma_{SL}}{\Delta S} \frac{dA}{dm}$$

$$\Rightarrow T - T_0 = - \frac{T_0 \gamma_{SL}}{\Delta H} \frac{dA}{dm}$$

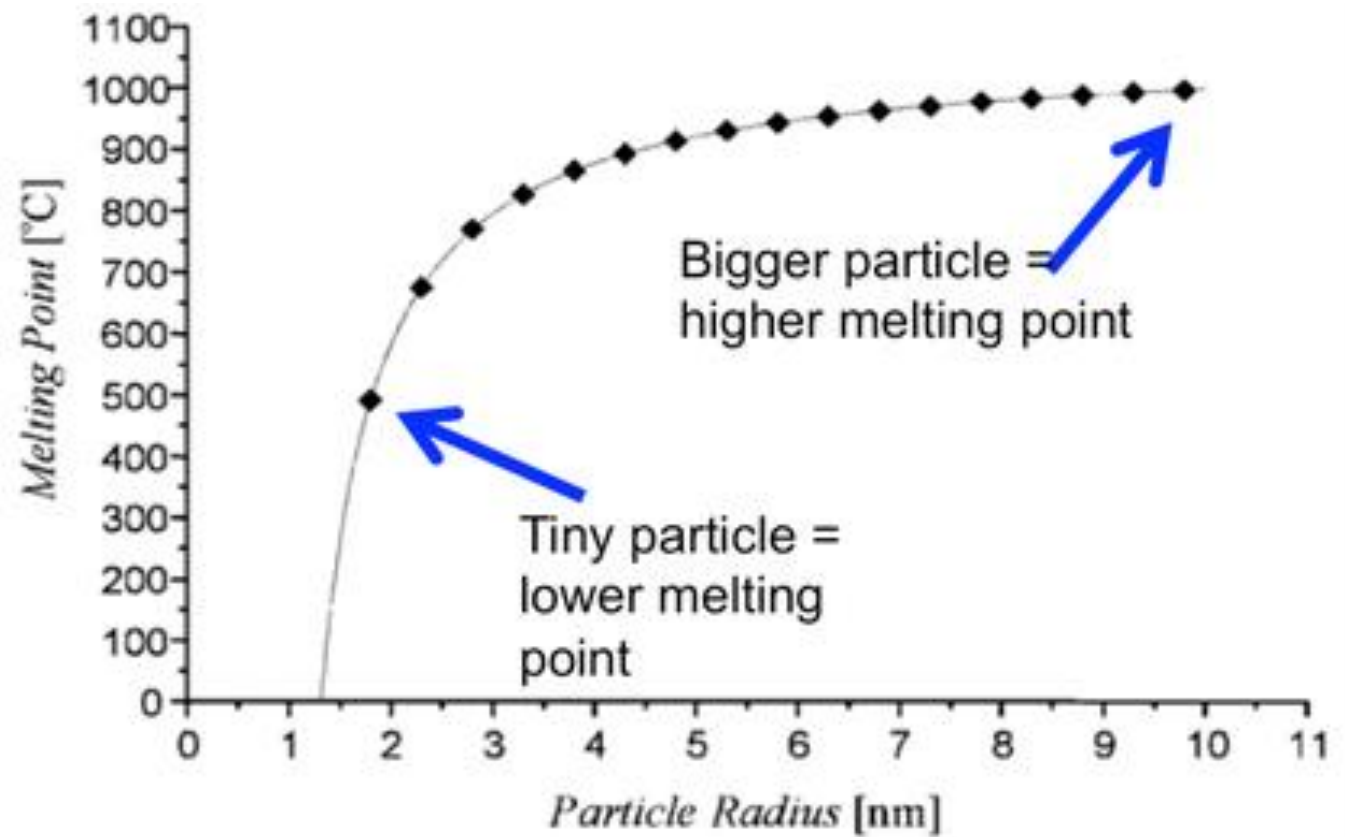
$$\Rightarrow T - T_0 = - \frac{T_0 \gamma_{SL}}{\Delta H} \frac{d(4\pi r^2)}{d(\rho \cdot \frac{4}{3} \pi r^3)}$$

$$\Rightarrow \frac{T - T_0}{T_0} = - \frac{2\gamma_{SL}}{\Delta H \rho r}$$

$$\Rightarrow \frac{T - T_0}{T_0} = - \frac{V_m(s)}{\Delta H_m} \frac{2\gamma_{SL}}{r}$$

- A simple model calculation shows that *the depression in melting point,  $\Delta T$ , is inversely proportional to the particle radius.*
- For spherical nanoparticles, experimental data often showed a roughly linear dependence of  $T$  with  $1/r$  (indeed, a more insightful analysis and modeling reveals the dependence is monotonic but not linear and that different melting processes exist). We report in the following Figures.

**Figure 6:** Relationship between particle size and *melting point* of *gold nanoparticles*. (graph used with permission from Schmid & Corain (2003))

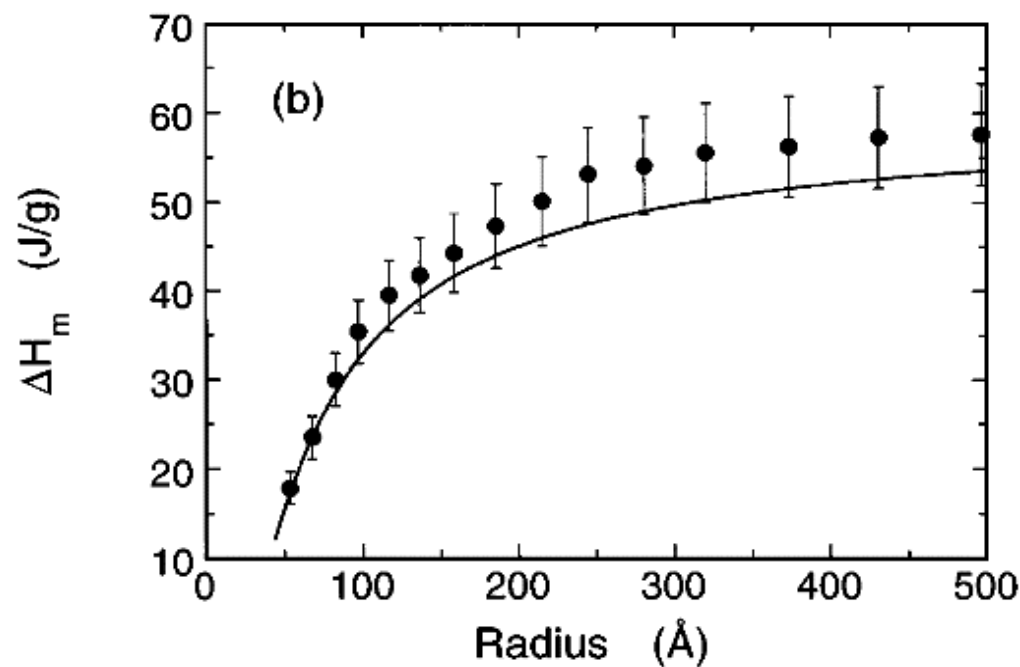
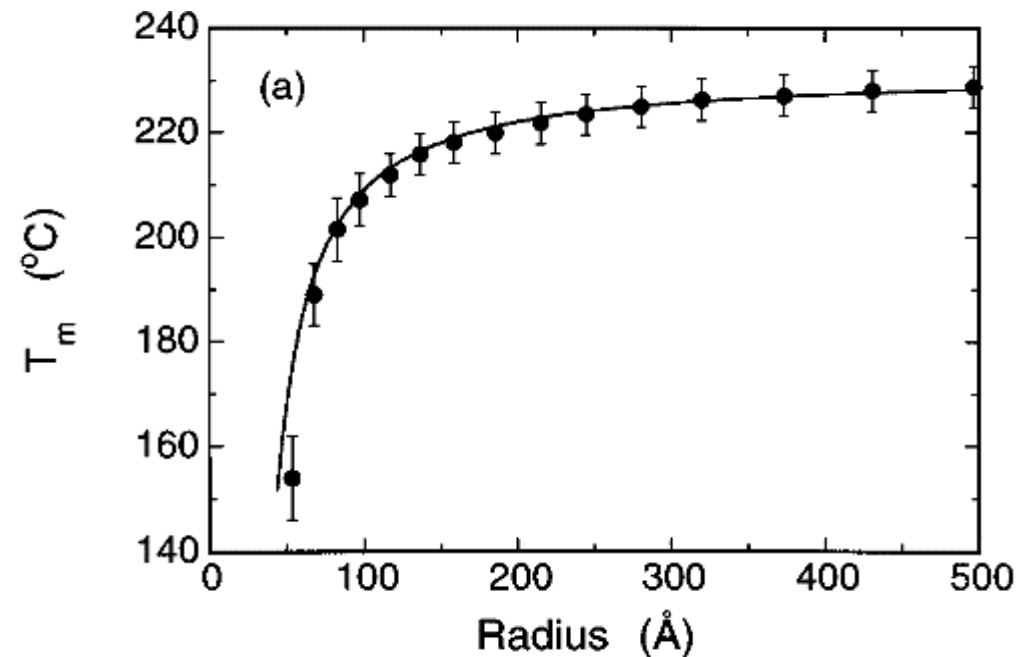


- Figure 6 shows the relationship between nanoparticle size and melting point for gold according to the Gibbs-Thomson equation. As we can see, *the melting point of gold nanoparticles can be even lower than room temperature (~23-25 °C) when the size decreases to less than about 1.4 nm*. At that size, there are only about 85 atoms present in each nanoparticle, and *most of the atoms are exposed on the surface*. (In contrast, in a 4 nm particle, there are nearly 2000 gold atoms, leaving most atoms still on the inside of the particle.)

**FIG. 2.** (a) *Size dependence* of the *melting points* of Sn particles.

(b) *Size dependence* of the normalized *heat of fusion*.

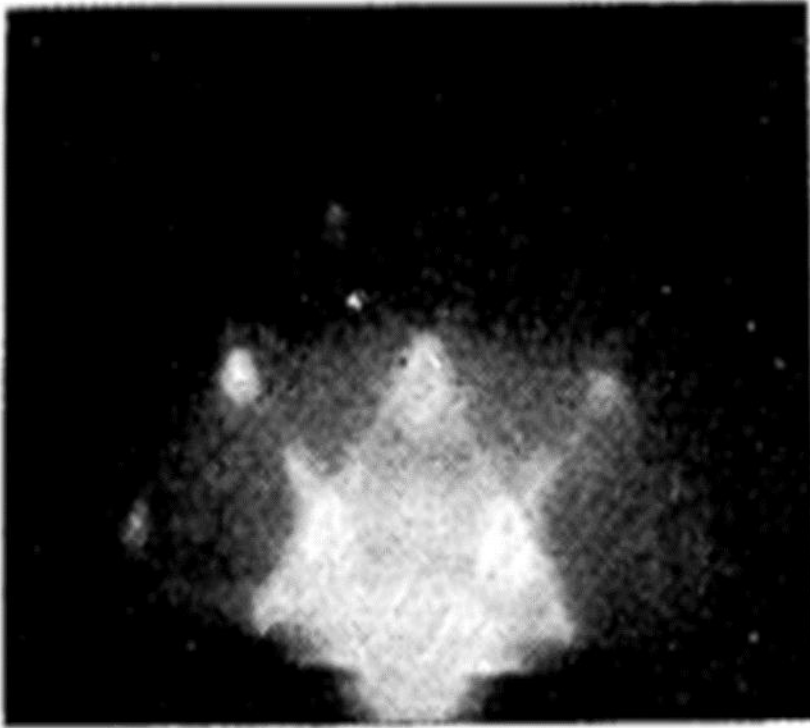
➤ *The heat of fusion  $\Delta H_m$  also decreases markedly from the bulk value.*



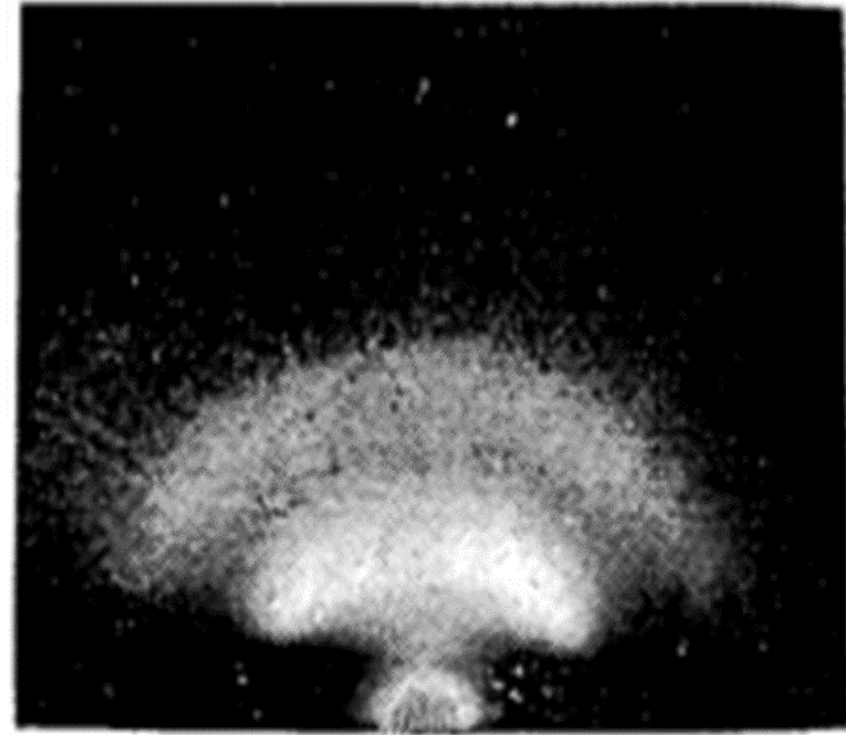
- The size dependence of the average melting temperature and normalized heat of fusion is plotted in Fig. 2. For bulk Sn, the melting point is 232 °C. It is evident that the melting points systematically decrease as the size of Sn particles decreases, a reduction of about 70 °C for Sn particles with  $r (avg) \sim 50 \text{ \AA}$ .
  - **Surprisingly**, the normalized *heat of fusion*  $\Delta H_m$  *also decreases markedly* from the bulk value which is 58.9 J/g by as much as 70% when the particle size is reduced [Fig. 2(b)]. From the **viewpoint of classical thermodynamics, the latent heat of fusion assumes a constant value.**
  - Not until recently have molecular-dynamics simulations shown a steady decrease of  $\Delta H_m$  with decreasing cluster size for Au clusters.
- ❑ *What is the **technique** for studying the **size-dependent melting point**...???*

- ❖ TEM is a standard *technique for studying the size-dependent melting point* depression phenomenon of small metal particles.
- When electron beams hit a sample, they can heat up and melt the nanoparticles. Atoms in a sample can also cause incident electron beams to diffract into many specific directions. By measuring the angles and intensities of these diffracted beams, diffraction patterns can be created and the position of the atoms in the sample can be determined.
- ✓ Atoms are generally highly ordered in solids but move around in liquids, which will result in different diffraction patterns.
- ✓ *Spotty patterns are usually observed for solid samples whereas halo patterns are usually observed for liquid samples. We can then differentiate solid state from liquid state by looking at their electron diffraction patterns.*
- ✓ At the melting point there is the change in the diffraction pattern associated with the disordering of the structure. However, as particle size decreases the diffraction technique becomes increasingly inaccurate due to line broadening. Moreover, TEM is limited to structural measurement only; it cannot measure the heat associated with the melting process. The ideal experimental technique for measuring melting of small particles is (*nano*)calorimetry.

solid state (spotty patterns)



liquid state (halo patterns)



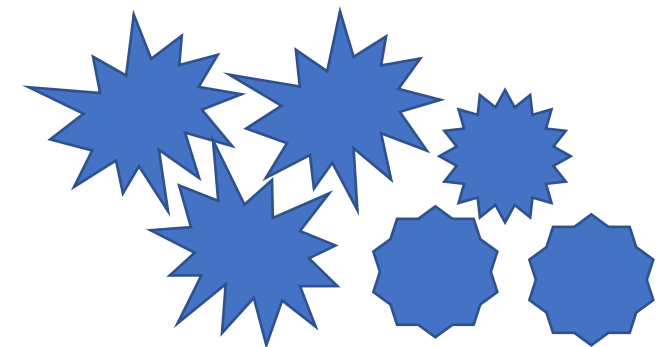
**Figure 8:** Diffraction pattern for *solid state* (spotty patterns, left) and liquid state (halo patterns, right) of lead.

(image reproduced with permission from JPSJ, Takagi (1954))



## ❑ *Sintering (Firing)*

- *Sintering is the process of pressing and heating of powdered materials close to their bulk melting point (but not **below** m.p.) for compacting the powder particles to create a solid shape.*
- The process creates materials with very uniform contents.
- Sintering is done in order to improve the mechanical, electrical and thermal properties of powdered materials.
- *Powdered materials have microscopically very rough surfaces and sharp tips. Such **nanoscale surface protrusions** have **melting temperatures well below their bulk melting temperature**.*
- *When the powdered particles are heated to high temperatures close to their m.p.s, the nanoscale **protrusions on the surface of the particles melt** (without melting the whole particle) and **diffuse to the neighbouring particles**. This leads to the reduction of the surface energy by decreasing the solid–vapor interface.*
- On cooling the powders solidify and form one solid mass.



## ❖ *Solubility Increases with Decrease in Particle Size*

- Consider spherical particles of radius  $r$  at constant temperature and pressure in equilibrium with *their saturated solution phase*. The criteria for equilibrium can be expressed by an equation analogous to solid-liquid equilibrium equation where the chemical potential of the melted particle,  $\mu_L$ , is here replaced by the chemical potential of the particle molecules in solution,  $\mu_P(sol)$ :  $\mu_P = \mu_P(sol)$ .

$$\text{➤ } \mu_S + \frac{2\gamma_{SL}}{\rho r} = \mu_P(sol)$$

- In the *case of a bulk solid phase*, instead, *the surface term is negligible*, and the above equation reduces to:

$$\mu_S = \mu_S(sol).$$

- *Merging of the above two equations* allows for **comparing the chemical potential of the molecules in solution in equilibrium with the particle** and to **the chemical potential of the molecules in equilibrium with the bulk solid phase**:

$$\mu_P(sol) - \mu_S(sol) = \frac{2\gamma_{SL}}{\rho r}$$

- Indeed, not a surprise at this point, *the difference results proportional to  $1/r$* .
- In the case of **diluted solution**, the chemical potential can be expressed as a function of the solute mole fraction at saturation  $x$ , viz., the **solubility**, by the equation:

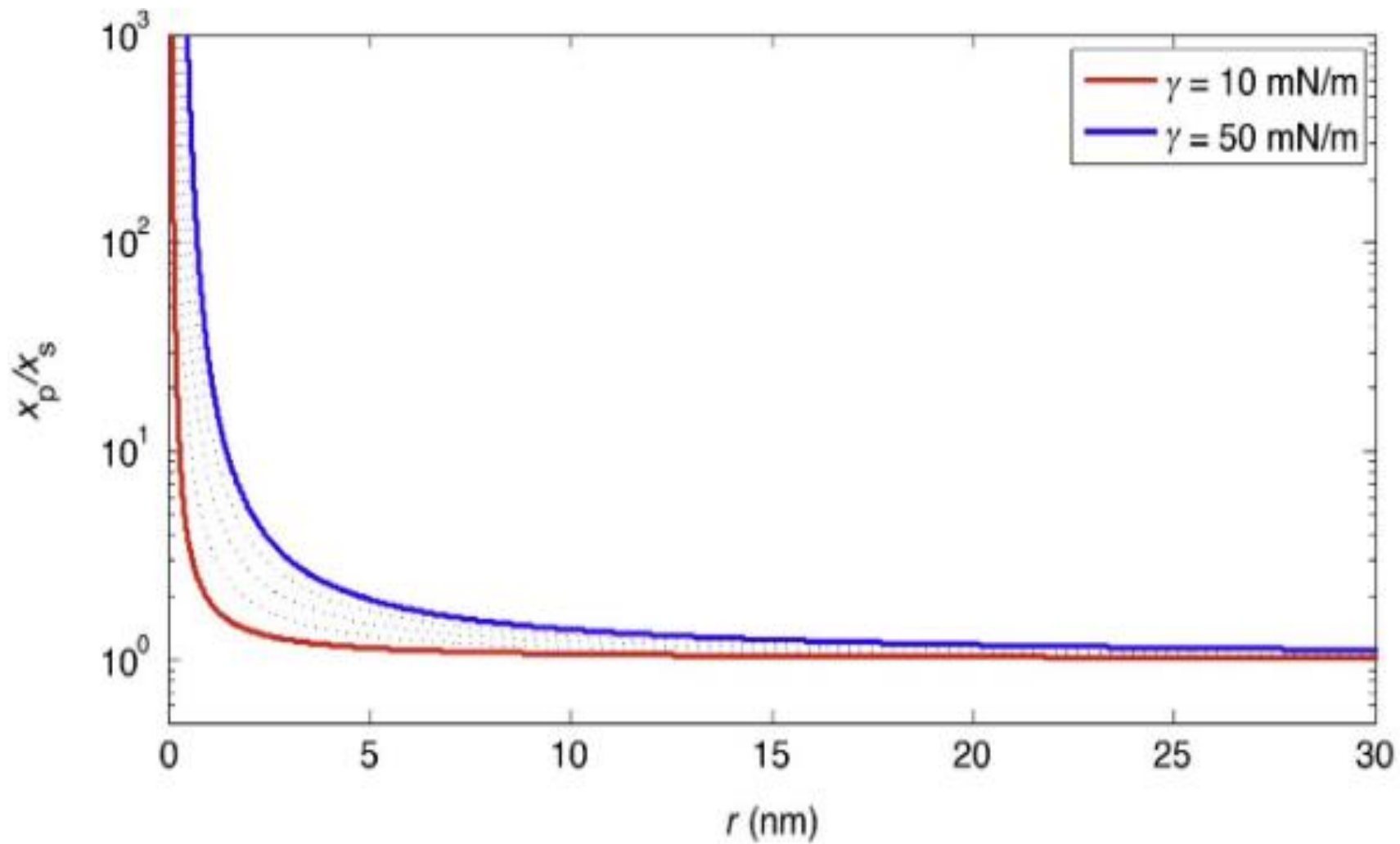
$$\mu_i(sol) = \mu^0 + RT \ln (x_i)$$

where  $\mu_i(sol)$  is the chemical potential of the molecules in solution in equilibrium with the particle or the bulk solid phase and  $\mu^0$  is the chemical potential of the solute molecules in the *bulk* standard state,  $R$  is the universal gas constant, and  $T$  is the Kelvin temperature.

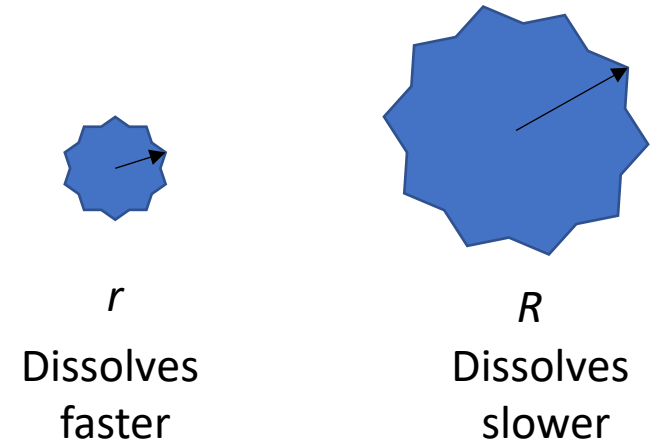
- By substituting the above equation in the former equation, one finally obtains

$$\ln \left( \frac{x_P}{x_S} \right) = \frac{1}{\rho RT} \frac{2\gamma_{SL}}{r} \quad (1:27)$$

- Equation (1.27) is the version of the **Ostwald-Freundlich relation** for a *spherical particle* solution system. It says that **spherical** particles have an **“excess” solubility that exponentially increases with the curvature  $1/r$** .



When  $r < R$  (for same  $\gamma$ )



**FIGURE 1.5** Increase of solubility of a *spherical particle* with respect to its *bulk solid phase* ( $x_p/x_s$ ) as a function of the particle radius ( $r$ ). The curves refer to a typical molecular solid with low (red line) and high (blue line) solid-solution interfacial tension ( $\gamma$ ).

- In Figure 1.5, we report the variation of  $x_p/x_s$  as a function of  $r$  for a typical molecular solid (molar mass equal to 350 g/mol and mass density equal to 1.25 g/cm<sup>3</sup>) with low and high solid-solution interfacial tension ( $\gamma_{SL}$ =10 and 50 mN/m, respectively) as predicted by Equation (1.27).
- *The “solubility excess effect” is more pronounced for high  $\gamma$  values*, for which it is detectable yet at  $r \approx 20$  nm.
- ✓ Instead, *for low  $\gamma_{SL}$  values,  $r$  must shrink to 5 nm in order to appreciate some effect.*
- We leave to the reader as a thought experiment the physicochemical interpretation of *why higher  $\gamma_{SL}$  implies the onset of solubility enhancement at higher  $r$ .*

## ❑ *Ostwald Ripening*

- Equation (1.27) suggests that *small particles are more soluble than their larger counterparts, viz., the smaller the particle is, the more the dissolution is energetically favored*. Thus, molecules passed into solution from smaller particles “prefer” to recondensate onto larger particles rather than coming back to the smaller ones. **This leads the larger particles to grow with time (in terms of both size and relative number) at the expenses of the smaller ones, which tend to shrink and fully dissolve, and to decrease the solute concentration in the solution.** *This peculiar time evolution of the particle size distribution is a well-established phenomenon known as “Ostwald ripening.”*
- It is ubiquitous in colloidal systems and has a primary role in determining their long-term stability. For example, *it is responsible of recrystallization of water within old ice cream*. As the ice cream shelf-life goes on, ice crystals *larger than some critical size enlarge* while smaller crystals dissolve, giving **old ice cream** *their inappropriate coarse texture* and *crunchy taste*.
- *Ostwald ripening, together with crystal nucleation and growth, is fundamental in several subjects of nanomaterials, from synthesis to long-term stability.*
- They are further peculiar examples of classical subjects of colloid and interface thermodynamics that are inherently “nano”.



## ❑ LOTUS EFFECT: SELF-CLEANING SURFACES

### ➤ Nanostructured SUPERHYDROPHOBIC Surfaces

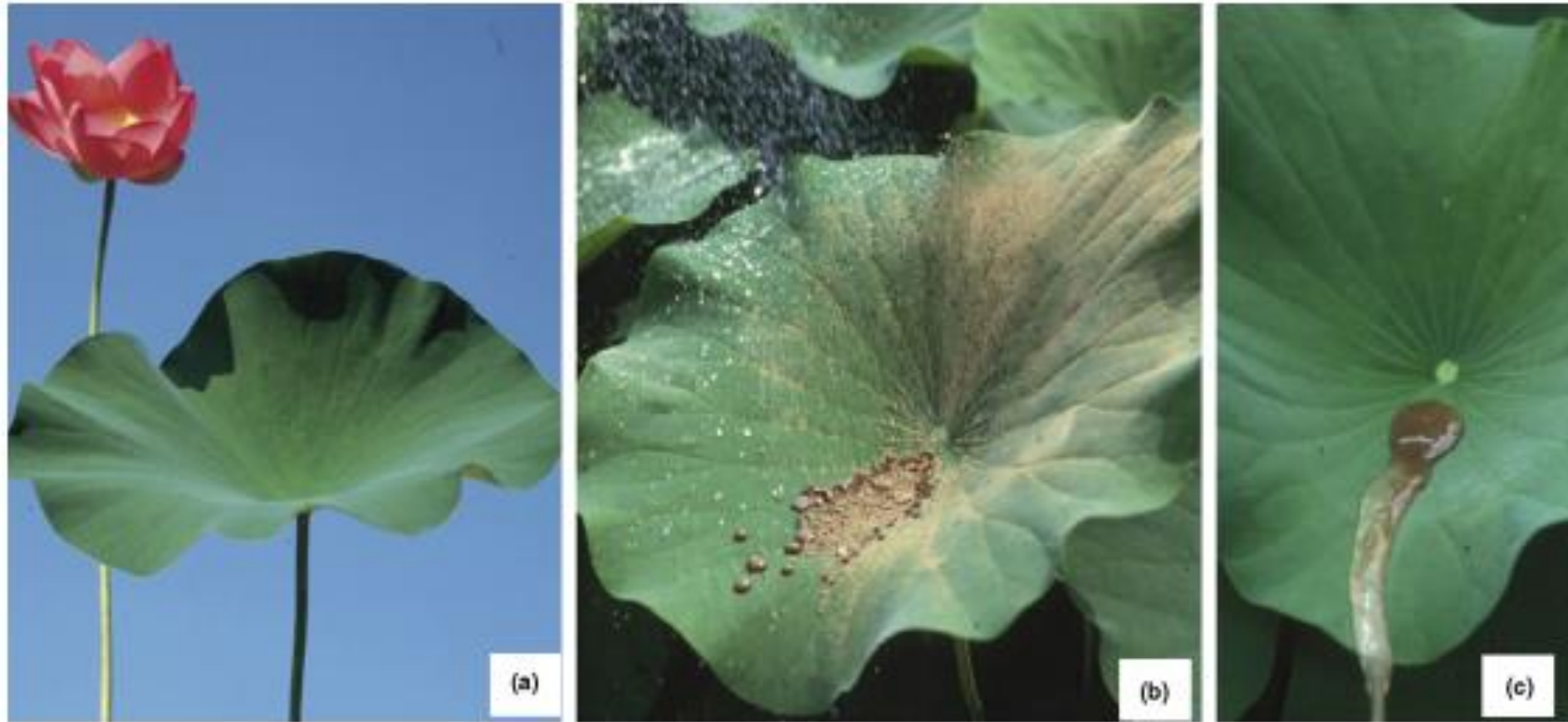


Fig. 3. Schematic illustration of lotus effect. (a-c) Lotus leaf: Water droplet beading on lotus leaf and self-cleaning.



# LOTUS EFFECT: Nanostructured **SUPERHYDROPHOBIC** Surfaces

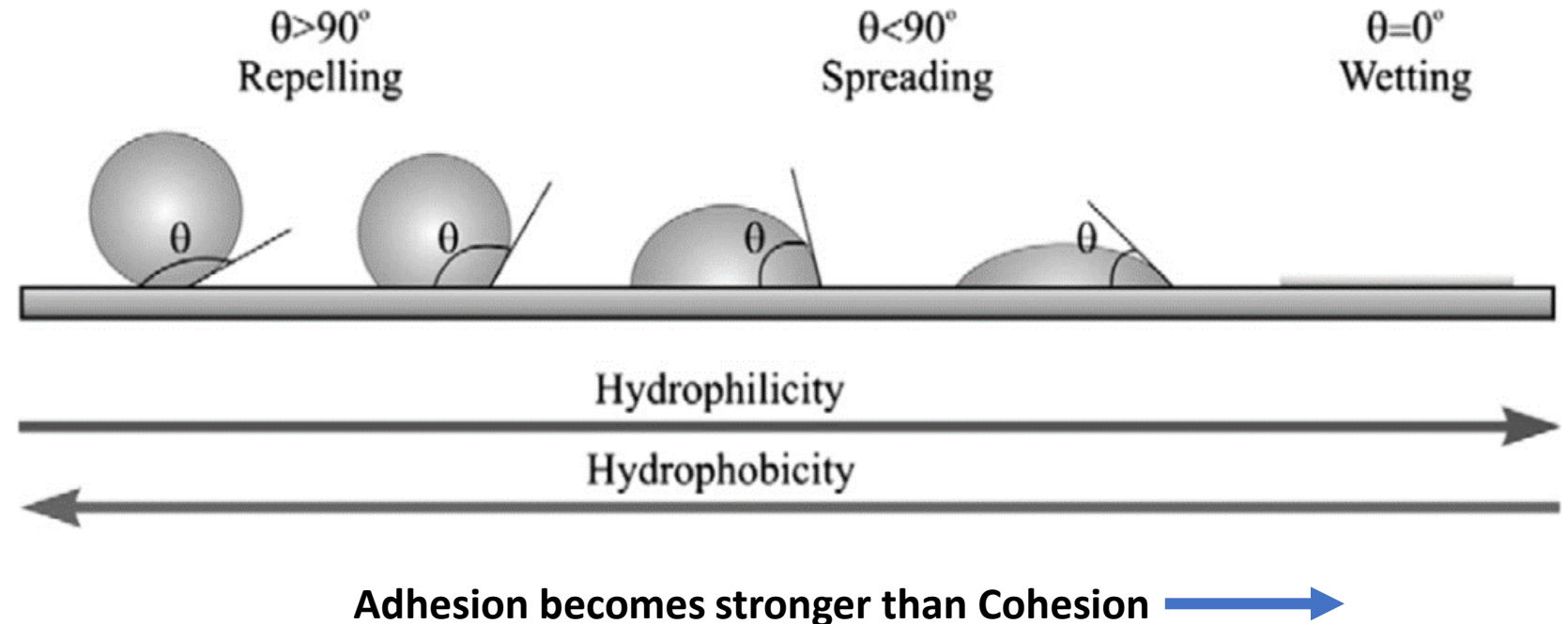
□ **Hydrophobic and Hydrophilic Surfaces: Wetting phenomena**



Lotus leaf: **Water droplet beading** on lotus leaf.

## ❑ Wetting phenomena: Hydrophobic and Hydrophilic Surfaces

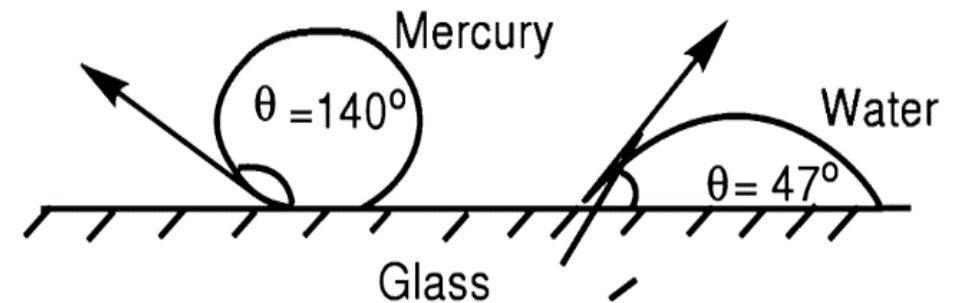
- ❖ A drop of liquid water placed on the surface of a solid:
  - *spreads* on the surface then shows *surface ‘wetting’* phenomenon or
  - *shrinks* on the surface then shows the “*nonwetting*” behavior.
  - *The wetting-nonwetting phenomena of a surface are usually determined by measuring the ‘contact angle’ (CA,  $\theta$ ) of water droplets on a surface.*



**Figure 1.** Schematic of *contact angle* (CA,  $\theta$ ) for a water drop placed on surfaces of different hydrophobicities.

- *A smaller contact angle implies a greater tendency to spread on the solid or equivalently, more wetting of the solid by the liquid.*
- *Note that a water drop that **completely wets a surface** will have a **contact angle of  $\sim 0^\circ$** , while a drop that has **no interaction with a surface (no wetting)** will **bead up into a perfect sphere (ignoring gravity)** and will have a contact angle of  **$\sim 180^\circ$** .*
- *Figure 2 compares a drop of mercury and a drop of water on a solid substrate such as glass. Mercury has a lesser tendency to spread or wet the glass surface.*

Fig. 2. A **drop of mercury** makes a larger contact angle ( $\theta = 140^\circ$ ) with glass than a **drop of water** ( $\theta = 47^\circ$ ).



➤ *A liquid will **not** wet the surface, if the cohesive force is much stronger than the adhesive force.*

❑ The contact angles between **water** and **some solids** are given in Table 2.3.

Table 2.3. Contact angles between water and some solid substrates

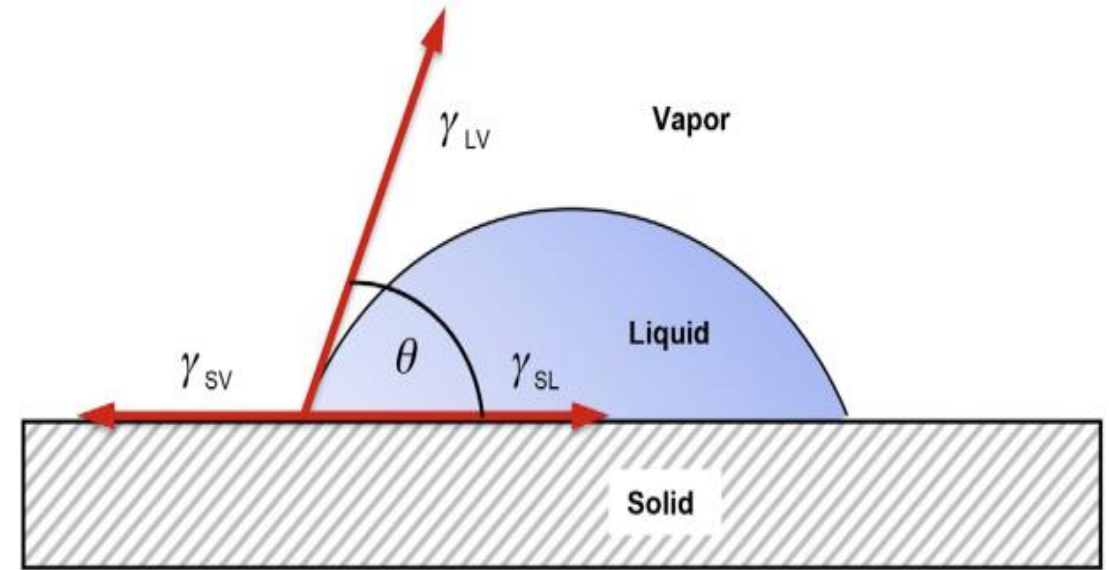
Substrate	$\theta$ (degrees)
Hydrated silica (SiOH on surface)	0
Gold	0
Silica	47
Graphite	85.7
Polyethylene	105
Paraffin wax	110
Teflon	115

- The contact angle for various systems varies between  $0^\circ$  and  $180^\circ$ .
- A value of  $\theta = 180^\circ$  for a liquid drop on a smooth surface is impossible because there is always some attraction between the liquid and the substrate.
- In practice, *the largest contact angle* achievable for water on a flat solid surface is  $\sim 120^\circ$  when the surface is *coated by a highly hydrophobic material such as fluorocarbon or silane*.
- For practical purposes, *if the CA is less than  $90^\circ$* , the surface is *conventionally* designated as *hydrophilic* (water-loving, wetting); if the *CA varies between  $90^\circ$  and  $150^\circ$* , the surface is designated as *hydrophobic*.

## Contact angle and Young's equation

- The '**contact angle (CA)**', ( $\theta$ ), is defined as the angle between liquid/gas interface and liquid-solid interface when a liquid droplet is placed on a solid surface.
- The contact angle ( $\theta$ ) measurement *assumes* a droplet is on a smooth, planar, and homogeneous surface.

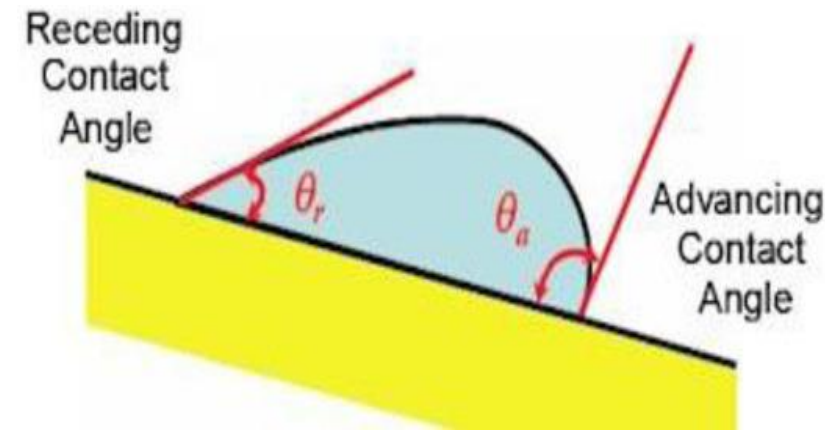
FIGURE 3 Illustration of the force diagram of Young's equation and contact angle. Liquid droplet on a smooth and homogeneous solid surface. The contact angle, CA, ( $\theta$  or  $\theta_Y$ ) and the solid-vapor ( $\gamma_{SV}$ ), the solid-liquid ( $\gamma_{SL}$ ), and the liquid-vapor ( $\gamma_{LV}$ ) interfacial tensions are evidenced.



- For a drop of liquid water ( $l$ ) in coexistence with a vapor phase ' $V$ ' that is put on a solid substrate ' $S$ ', the **Young's equation** describes the force balance between the interfacial tensions formed at the solid–liquid–vapor contact line at equilibrium:  $\cos\theta_Y = (\gamma_{sv} - \gamma_{sl})/\gamma_{lv}$   
 $\theta_Y$  = **Young's contact angle**;  $\gamma_{sv}$  = surface tension (energy per unit surface) of the solid–vapor interface;  $\gamma_{sl}$  = surface tension of the solid–liquid interface;  $\gamma_{lv}$  = surface tension of the liquid–vapor interface.
- This **equation is applicable only to flat and smooth** surfaces and **not to rough ones**.

□ In practice, **two types of CA values are used: static and dynamic.**

- *Static* CAs are obtained by sessile drop measurements, where **a drop is deposited** on the flat surface, and the value is *close* to the ideal  $\theta_Y$ .
- In practice, also, **out-of-equilibrium CAs are of interest and often measured.** These so-called **dynamic CAs** are measured during the growth (**advancing CA**,  $\theta_{ad}$  or  $\theta_a$ ) and shrinkage (**receding CA**,  $\theta_{rd}$  or  $\theta_r$ ) of the liquid droplet.
- Figure 4 shows a water drop on a tilted surface exhibiting advancing ( $\theta_a$ ) and receding ( $\theta_r$ ) contact angles.
- In general, **advancing CA ( $\theta_a$ ) exceeds receding CA ( $\theta_r$ ).** The **difference between  $\theta_a$  and  $\theta_r$**  is defined as **contact angle hysteresis ((CAH,  $\Delta\theta$ )).**



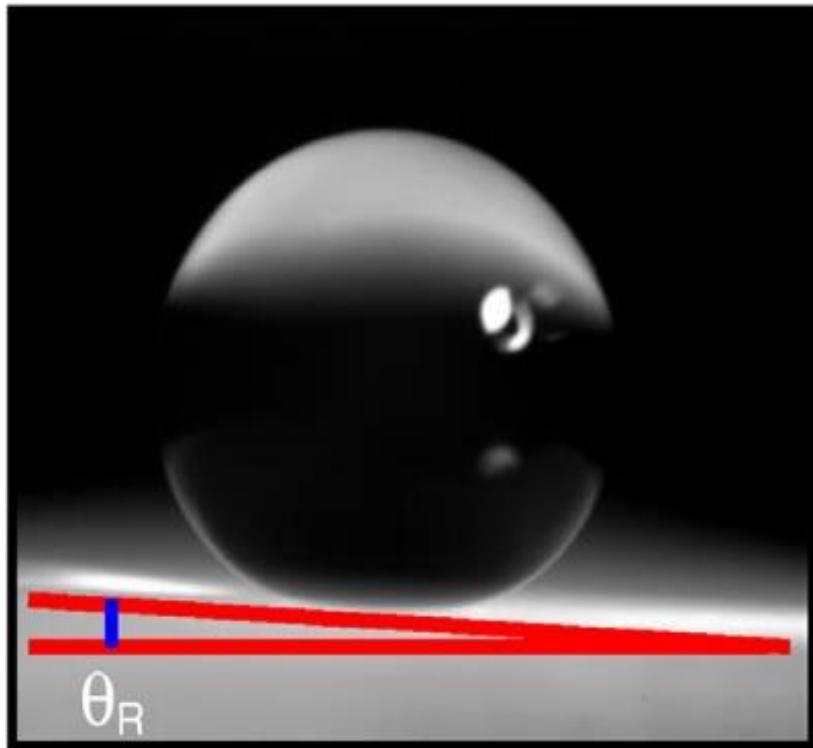
**Figure 4.** Advancing and receding dynamic contact angles.



- CA hysteresis (CAH) can arise, from **molecular interactions** between the liquid and the solid surface as well as from **surface roughness** and **heterogeneity**.
- The values of  $\Delta\theta$  *can be as low as  $10^\circ$  on crystalline silicon*, while many surfaces show much *larger hysteresis due to chemical heterogeneity and roughness*.
- Finally, it is worth noting that the *experimental values of CA* should be more properly called *“apparent CAs”* because, due to the “imperfections” of real surfaces, the measured CA values never match  $\theta_Y$ , and, depending on the imperfection, it may be similar or exceptionally different from it.

## ❑ *Roll-off Angle ( $\theta_R$ or $\alpha$ )*

- *The angle at which a water drop rolls off a tilted flat surface is known as the **roll-off angle** ( $\alpha$  or  $\theta_R$ ).*
- *Generally, **superhydrophobic** surfaces exhibit roll-off angles of less than 5 degrees, but very **high quality superhydrophobic surfaces** can exhibit roll-off angles of less than 1 degree.*
- *Figure 5 shows a water drop with a roll-off angle of ~5 degrees.*



**Figure 5.** Water drop roll-off angle.

- *Hydrophobicity is usually determined by measuring the CA of water droplets on a surface. The **contact angle hysteresis** is more important in **determining hydrophobicity** than the maximum achievable static contact angle.*
- *A water droplet on a surface with a large static contact angle may remain pinned until the surface is tilted to a significant angle, and the difference between dynamic contact angles (advancing  $\theta_{ad}$  and receding  $\theta_{rc}$  contact angles) *presents a clear indication of how stable the water droplet is on that solid surface.**
- The following equation describes the force needed for a water droplet to start moving over a solid surface

$$F = \gamma_{LV}(\cos \theta_{rc} - \cos \theta_{ad})$$

where  $\gamma_{LV}$  is the water surface tension.

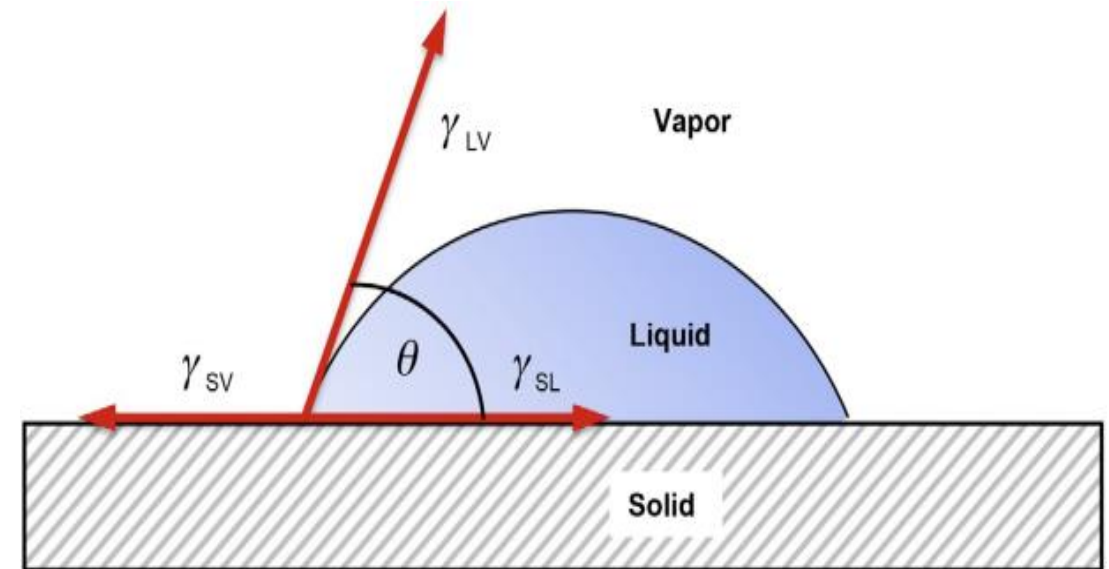
- As mentioned in the previous sections, *a low CAH allows water to roll off easily* along the surface.
- In the case of **perfect hydrophobicity** ( $\theta_{ad}/\theta_{rc} = 180^\circ/180^\circ$ ), the spherical drop touches the surface at a single point and moves readily on the surface.

- **Contact Angle Hysteresis:** The difference between advancing and receding contact angles is referred to as the *contact angle hysteresis (CAH)*.
- ✓ According to the difference in contact angle hysteresis, surfaces can perform as *slippery or sticky surfaces*. The pinning phenomenon during the evaporation of a droplet is an example of the contact angle hysteresis.
- **Superhydrophobic surface:** When the *effective contact angle of water drops is  $150^\circ$  or higher*, in addition to *a low CAH ( $<10^\circ$ )*, and the *roll-off angles of less than 5 degrees*, the surface is defined as **superhydrophobic**.
- ✓ **Superhydrophobic surfaces** play an important role in *many applications, such as contamination prevention, enhanced lubricity, and durability of materials*.
- **Ultrahydrophobic surface:** A surface that exhibits both advancing and receding contact angles of greater than  $150^\circ$ .

## Contact angle and Young's equation

- The contact angle ( $\theta$ ) measurement assumes a droplet is on a smooth, planar, and homogeneous surface.
  - For a drop of liquid water ( $l$ ) in coexistence with a vapor phase ' $V$ ' that is put on a solid substrate ' $S$ ', the **Young's equation** describes the force balance between the interfacial tensions formed at the solid–liquid–vapor contact line at equilibrium:  $\cos\theta_Y = (\gamma_{sv} - \gamma_{sl})/\gamma_{lv}$
- $\theta_Y$  = **Young's contact angle**;  $\gamma_{sv}$  = surface tension (energy per unit surface) of the solid–vapor interface;  $\gamma_{sl}$  = surface tension of the solid–liquid interface;  $\gamma_{lv}$  = surface tension of the liquid–vapor interface.
- This equation is *applicable only to flat and smooth* surfaces and *not to rough ones*.

FIGURE 3 Illustration of the force diagram of Young's equation and contact angle. Liquid droplet on a smooth and homogeneous solid surface. The contact angle, CA, ( $\theta$  or  $\theta_Y$ ) and the solid-vapor ( $\gamma_{sv}$ ), the solid-liquid ( $\gamma_{sl}$ ), and the liquid-vapor ( $\gamma_{lv}$ ) interfacial tensions are evidenced.



## ❑ Effects of *Surface Roughness* or *Topology* on *Contact Angle*

- The *apparent water contact angle of smooth surfaces* ( $\theta_Y$ ), described by the Young equation, depends on the solid–vapor, solid-liquid, and liquid-vapor surface tensions and *does not exceed 125–130°*, whatever the surface chemistry.
- However, *many natural surfaces display superhydrophobic properties*.
- ✓ Such properties are characterized by an apparent water contact angle ( $\theta_Y$ )  $> 150^\circ$  and various adhesions of water on the surface determined by *dynamic contact angle measurements* (CA hysteresis and *sliding angle*  $\alpha$ ).
- *Intensive surface analyses at the micro and nanoscale have shown the necessity of surface structures.*
- *The surface energy of a solid is determined by surface chemistry*, which in turn depends on the *chemical composition and atomic arrangements at or near the surface*.
- *The water–solid contact angle varies with the surface energy and roughness of the solid surface.*

- Occurrence of **contact angle hysteresis** is associated with **the *surface defects***, which could be from the *surface roughness*, *chemical heterogeneity*, or wetting state.
- Structure relaxation, surface restructuring, and composition segregation all can *reduce the surface energy and, thus, result in an increase in contact angle*. However, such *a reduction in surface energy would result in a limited increase in contact angle and is insufficient to make a surface superhydrophobic*.
- Usually trifluoromethyl carbon ( $-\text{CF}_3$ ) containing diblock polymers, surfactants, or coupling agents are self-assembled on the solid surface to form a monolayer. Surfaces terminated with trifluoromethyl carbon ligands possesses highest electron–fluorine affinity and consequently the lowest surface energy.
- *Contact angle decreases when the  $-\text{CF}_3$  monolayer is less than close-packed, but even on the fully packed monolayers, contact angle on a smooth surface generally does not exceed  $120^\circ$ .*
- **A further increase in contact angle and hydrophobicity, will require an increase in surface roughness.**



# ❑ LOTUS EFFECT: NANOSTRUCTURED SUPERHYDROPHOBIC Surfaces

## ❖ Effects of *Surface Roughness* or topology on *Contact Angle*

- If a liquid water drop is placed on a flat, smooth, homogeneous surface (substrate), its localized contact angle will strictly be a function of the liquid's surface tension and the surface's chemistry (surface energy). Thus, the *Young equation was based on the concept of an idealized, atomically smooth solid surface.*
- However, *all surfaces have defects and imperfections, which could be from surface roughness, chemical heterogeneity*, etc. The *surface roughness and heterogeneity* will contribute to the surface wetting behavior.
- The *effective contact angle will either decrease or increase*, depending on the substrate's surface chemistry.
- The **effect of the surface structure on the wettability (contact angle)** has been explained by two well-established models: the **Wenzel model** and the **Cassie-Baxter model**.

## ❑ *Wenzel and Cassie–Baxter regimes*

- *The change in effective contact angle as a result of surface roughness and structure heterogeneity falls into two regimes, known as the Wenzel and Cassie–Baxter regimes.*
- *The Wenzel model proposes how contact angle change arises from a larger area of contact as the surface area is increased from the smooth to the structured surface even when the projected area is the same.*
- *While both regimes describe how a change (increase) in contact angle happens with increasing surface roughness, the Cassie–Baxter regime comes into effect when there is a trapped air layer within the roughened or textured surface which causes a substantial increase in contact angle and a significant reduction in roll-off angle and contact angle hysteresis.*
- *Indeed, among all the factors, roughness exerts the greater influence on apparent CA.*
- *The behavior of a liquid droplet on a rough surface is schematically shown in Figure 1.8. The liquid can either penetrate the asperities (Figure 1.8, left) or stay suspended above them (Figure 1.8, right). In both cases, different apparent CAs are observed with respect to the one that could be observed on the corresponding ideal flat surface.*

- These two situations are named the *Wenzel state* and the *Cassie-Baxter state*, after the names of the scientists that introduced the models (in the 1940s). *These models set the frame for the description of superhydrophobic surfaces (SHSs).*

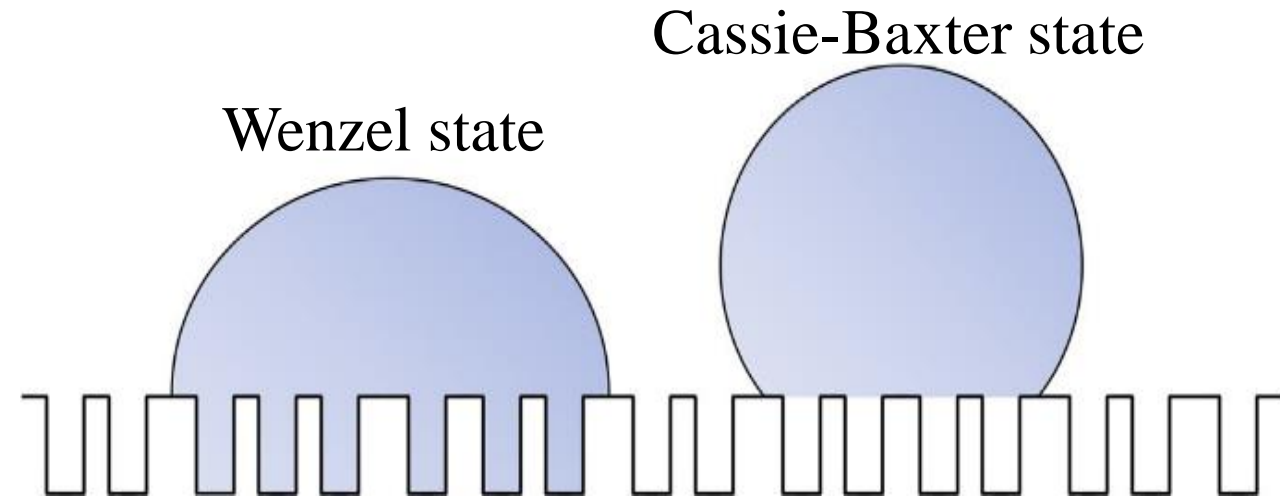


FIGURE 1.8 Behavior of a liquid droplet on a rough surface.

Left Drop: Wenzel state;  
right drop: Cassie-Baxter state.

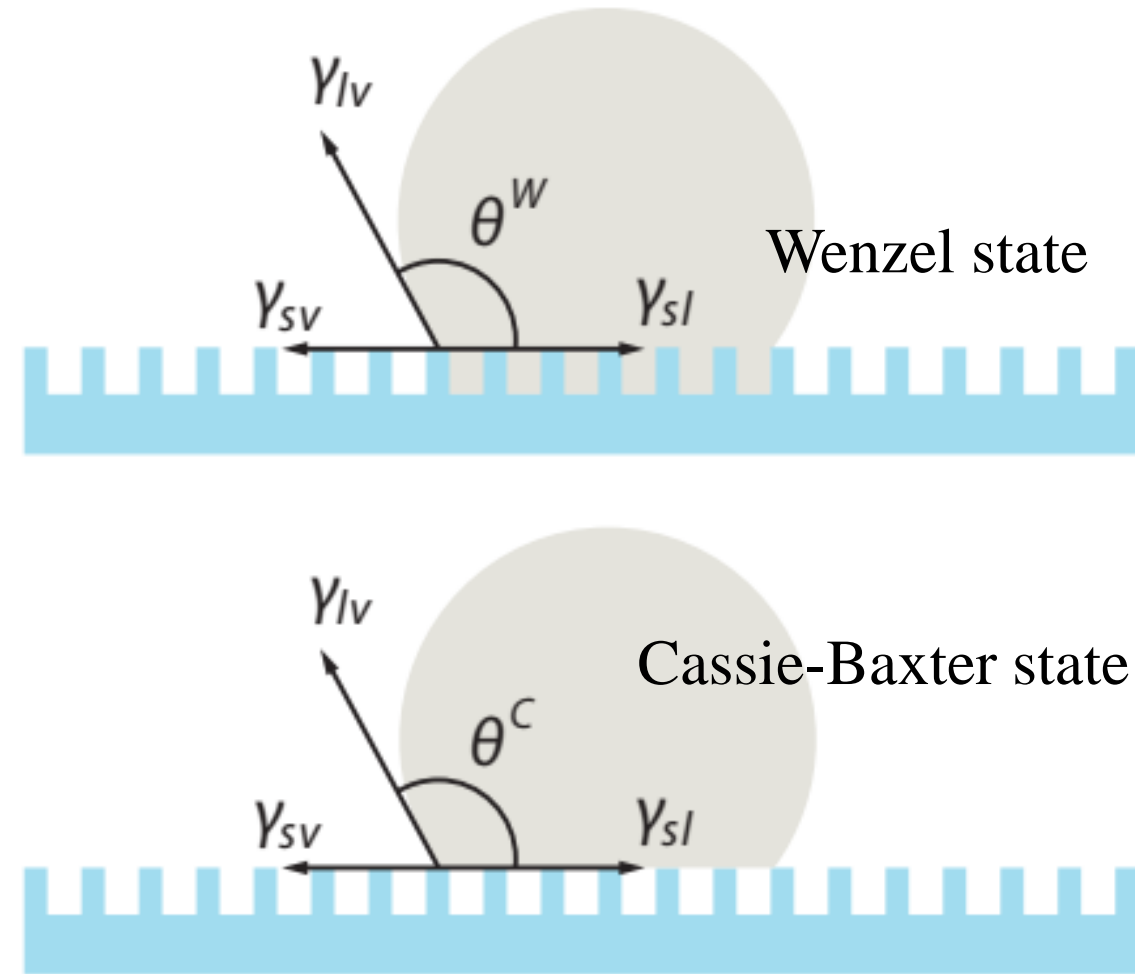


Figure 7.15: Illustration of the Wenzel and Cassie models of increased hydrophobicity on structured surfaces.

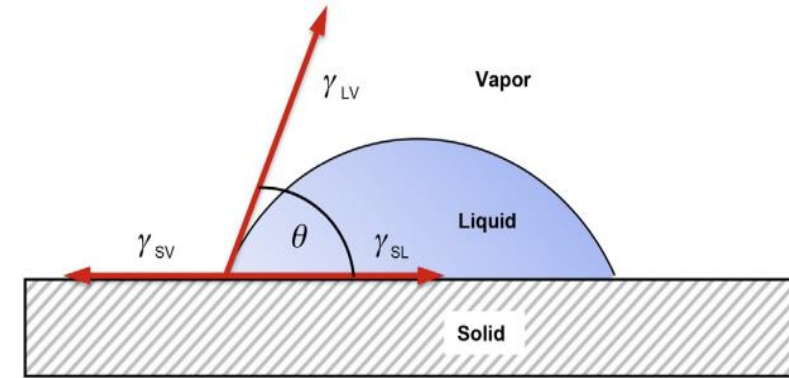
- On **rough surfaces**, the Young equation no longer applies. Wenzel (1936, 1949) proposed a model to describe the **apparent contact angle,  $\theta_W$ , with a rough surface**, by relating it to that with a flat surface  $\theta_Y$ .
- The **basic assumption** in Wenzel's theory is that the **liquid follows the roughness of the surface and fills the asperities**. He modified the Young equation by introducing a solid **surface roughness factor,  $r$** , as follows:

$$r \gamma_{sv} = r \gamma_{sl} + \gamma_{lv} \cos \theta_W$$

- Upon rearrangement, one gets:  $\cos \theta_W = r (\gamma_{sv} - \gamma_{sl}) / \gamma_{lv}$

- In other words,  $\cos \theta_W = r \cos \theta_Y$  (1:39)

- **This is called the Wenzel equation.** Here  $\theta_W$  corresponds to the *apparent CA*, in the Wenzel state, **on a rough solid surface**;  $r$  represents the roughness factor; and  $\theta_Y$  is the Young's CA (also referred as *intrinsic CA*).
- Thus, **at equilibrium**, there is a **linear relationship between the apparent CA ( $\theta_W$ ) and the roughness factor of the surface**.



➤ The **roughness factor,  $r$** , is the *nondimensional* surface roughness factor is defined by *the ratio* of the *actual* surface area of a rough surface ( $A_{Rough}$ ) to the *projected* surface area (assuming *flat projected area*) ( $A_F$ ).

$$\cos \theta_W = r \cos \theta_Y$$

$$r = \frac{A_{Rough}}{A_F}$$

- Therefore, *for a rough surface,  $r > 1$* .
- Since  $r > 1$ , the roughness on a *hydrophobic surface* (where  $\theta_Y > 90^\circ$ ) *increases the contact angle* ( $\theta_W$ ) and *renders the surface more hydrophobic*.
- **On the contrary**, for a *hydrophilic surface* (with  $\theta_Y < 90^\circ$ ), *roughness has the opposite effect*. Because for  $\theta_Y < 90^\circ$ , *an increase of  $r$  leads to a decrease of  $\theta_W$* , toward  $0^\circ$  and yielding a *more hydrophilic surface*.
- ✓ Therefore, if the surface chemistry is *hydrophilic*, then *roughening its surface will decrease its CA*.
- ✓ If the surface is *hydrophobic*, then *roughening its surface will increase its CA*.
- Therefore, *roughness may enhance either hydrophilicity or hydrophobicity*, depending on the chemistry of the corresponding flat surface.

$\theta$	$\cos \theta$	$\sin \theta$
0	1	0
$\frac{\pi}{6}$	$\frac{\sqrt{3}}{2}$	$\frac{1}{2}$
$\frac{\pi}{4}$	$\frac{\sqrt{2}}{2}$	$\frac{\sqrt{2}}{2}$
$\frac{\pi}{3}$	$\frac{1}{2}$	$\frac{\sqrt{3}}{2}$
$\frac{\pi}{2}$	0	1
$\frac{2\pi}{3}$	$-\frac{1}{2}$	$\frac{\sqrt{3}}{2}$
$\frac{3\pi}{4}$	$-\frac{\sqrt{2}}{2}$	$\frac{\sqrt{2}}{2}$
$\frac{5\pi}{6}$	$-\frac{\sqrt{3}}{2}$	$\frac{1}{2}$
$\pi$	-1	0

- Note that *a hydrophilic surface becomes more hydrophilic, and a hydrophobic surface becomes more hydrophobic when the given surface is roughened*, or its topography is significantly increased.
- However, it has been demonstrated that **CA hysteresis (CAH)** on hydrophobic surfaces *increases with increasing surface roughness in the low-roughness region but drastically decreases when the roughness becomes large and the composite configuration, in which the liquid does not penetrate the asperities, is energetically advantageous.*
- ✓ *This decrease in CA hysteresis is attributed to switching from the Wenzel to the Cassie-Baxter state.*
- This happens because higher  $r$  implies the *fraction of vapor* trapped between the liquid and the pockets determined by the surface protrusions (roughness) is enough to drive the suspension of the droplet on top of the asperities, as shown in the Figures above.
- ✓ In simpler words, *the liquid drop starts to see the surface as the vapor phase and therefore strives to become spherical.*



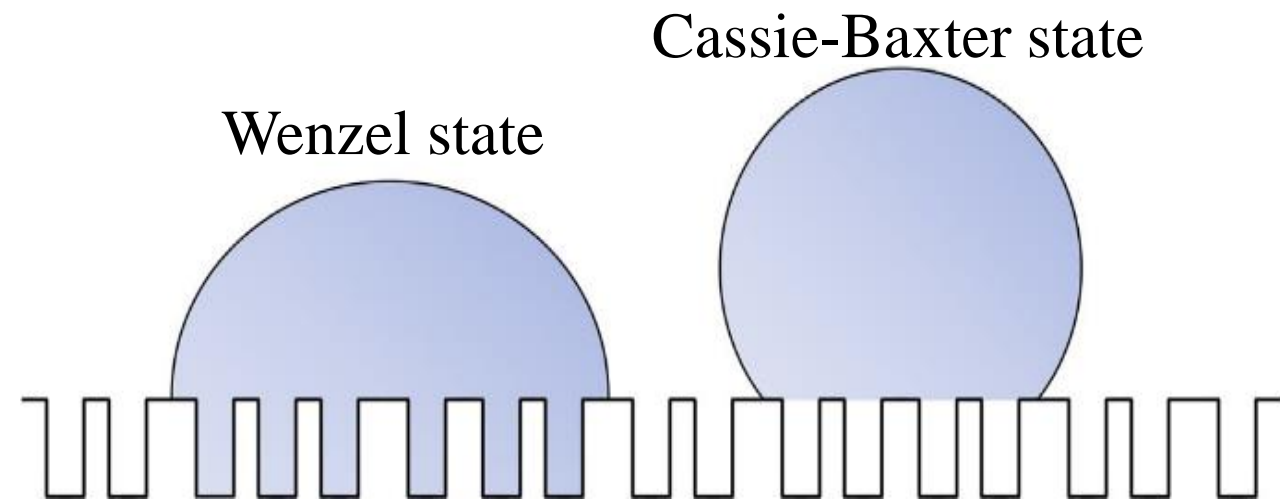


FIGURE 1.8 Behavior of a liquid droplet on a rough surface.

Left Drop: Wenzel state;  
right drop: Cassie-Baxter state.

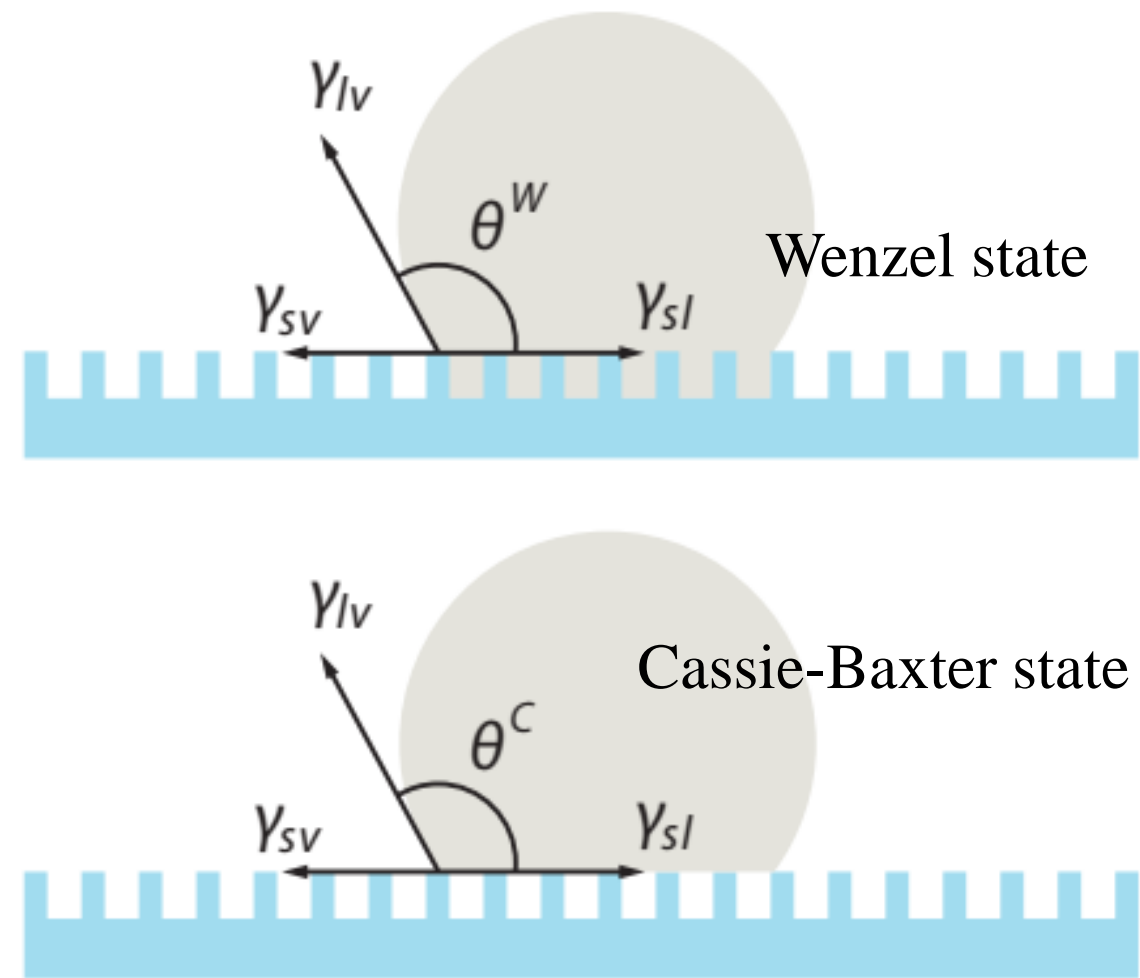


Figure 7.15: Illustration of the Wenzel and Cassie models of increased hydrophobicity on structured surfaces.



➤ The suspension of the liquid droplet can be therefore described as a composite state. As a result, *in the Cassie-Baxter model* (1944), *the apparent CA is the results of the sum of the contributions from both the solid phase and the (trapped) vapor phase* and is described by

➤ 
$$\cos \theta_{CB} = f_1 \cos \theta_{Y1} + f_2 \cos \theta_{Y2} \quad (1:40)$$

where  $\theta_{CB}$  is the apparent CA, in the Cassie-Baxter state, on a rough surface;  $f_1$  and  $f_2$  are the *surface fractions of phases 1 and 2* in contact with the liquid, respectively (and  $f_1 + f_2 = 1$ ); and  $\theta_{Y1}$  and  $\theta_{Y2}$  are the Young's CAs of phases 1 and 2, respectively.

➤ Say, here  $f_1$  and  $f_2$  are the *area fractions* of the **solid** and the **vapor in contact with the liquid**.

➤ That is, for a rough surface featuring a single type of asperity, if  $f_s$  is the *fraction* of solid surface in contact with the liquid ( $f_1$ , where  $0 < f_1 < 1$ ), then the vapor fraction,  $f_2$ , is  $(1 - f_s)$ .

➤ *If the liquid is water and the vapor is **air**, then  $\theta_{Y2} = 180^\circ$* , (and  $\theta_{Y1} = \theta_{YS}$ ) and the resulting CA (from Equation 1:40 above) can be calculated by the following equation:

$$\cos \theta_{CB} = f_s \cos \theta_{YS} + (1 - f_s) \cos \theta_{Y2} = f_s (\cos \theta_{YS} + 1) - 1 \quad (1:41)$$

➤ Thus, in the above **Cassie-Baxter** eqn.,  $\theta_{CB}$  is the sole function of the solid  $f_s$  and  $\theta_{YS}$ .

- From the Cassie-Baxter eqn., it can be noticed that *a decrease in the solid fraction ( $f_s$ ) and an increase in the air fraction would enhance the water repellency* of a *surface regardless of whether the surface is hydrophobic or hydrophilic*.
- The *model proposes that the increased contact angle arises because air is trapped within the structures on the surface*, and since the air-liquid contact angle will be close to  $180^\circ$ , *the contact angle will increase in proportion to the fraction of the drop in contact with the trapped air* rather than the hydrophobic surface.
- The *two equations (Wenzel and Cassie-Baxter) describe two limiting behaviors*. However, *surfaces may often show intermediate Wenzel-Cassie state*. In these cases, **the apparent CA,  $\theta_a^r$ , depends on both the fraction and the roughness of the solid surface:**

$$\cos \theta_a^r = r f_s \cos \theta_{YS} + f_s - 1$$

- For many surfaces, a transition from Cassie-Baxter to Wenzel state was observed. Many factors can determine this change such as surface *chemical heterogeneity and roughness*.

- It has been argued that these models probably represent different limits of behavior, where the *Wenzel model is most likely to hold for slightly hydrophobic surfaces*, i.e., when the contact angle is between  $90^\circ$  and some larger angle,  $\theta_T$ , where there would be a transition to the behavior described by the Cassie model. In that case, the angle at which the transition in behavior occurs can be calculated by equating Equation 1.39 and 1.40 to give

$$\cos\theta^T = \frac{f - 1}{r - f},$$

which yields a transition angle between  $90^\circ$  and  $180^\circ$  as expected.

- *When the surface contains nanostructures, the expectation is that either the ratio,  $r$ , is very large, or the fraction,  $f$ , is very small.*
- Assume  $r=1.5, f=0.01$ , then calculate the angle  $\theta^T$ .
- In either case, we expect to be beyond the transition angle, and we would apply the Cassie model to give a very high contact angle. Such nanostructured surfaces are said to be *superhydrophobic or ultrahydrophobic*.

- *The idea is conceptually straightforward; increased roughness will result in an increase in true surface area and, thus, lead to an increased nominal surface energy.*
- *Accordingly, the contact angle varies as dictated by Young's equation.*
- *It has been demonstrated that the contact angle will increase with increased roughness of a hydrophobic surface, whereas the contact angle will decrease with increased roughness of a hydrophilic surface. **This relationship was established by Wenzel and referred to as Wenzel's law.***
- *However, Young's equation and Wenzel's law **can only be used** if the water droplet has **complete contact** with the rough surface.*
- *In reality, the contact between water and a hydrophobic rough surface cannot reach 100% and some air bubbles will be trapped at the interface. *One can see that two interfaces are attributed to the contact between a droplet and a rough surface.**
- *One is the interface between the droplet and the solid surface, and the other is the interface between the droplet and trapped air bubbles. Consequently, Cassie-Baxter equation should be applied.*
- ***From the Cassie-Baxter equation one finds that the more air trapped between the rough surface and the water, the larger the contact angle will be.***

- Interestingly, the *mobility of the drop on the surface is expected to be quite different* for the two models. The *Wenzel model* would predict that the drop would be pinned to the surface by the large contact area, and it would require a high tilt angle for the drop to move across the surface.
- On the other hand, the *Cassie-Baxter model* would predict that as the contact fraction,  $f_s$ , decreases, the *drop should become more mobile* on the surface.
- According to the *Wenzel state*, the water droplet is in complete contact with the surface and  $\theta_Y$  is amplified by a roughness parameter ( $r$ ). *Superhydrophobic properties can be reached only if  $\theta_Y > 90^\circ$  (intrinsically hydrophobic materials), but with high CA hysteresis and  $\alpha$  due to the increase in the solid–liquid interface.*
- According to the *Cassie–Baxter* equation, the water droplet is suspended on a composite interface made of solid and air trapped between the droplet and the surface. *The Cassie–Baxter equation can predict superhydrophobic properties but with low CA hysteresis and  $\alpha$  due to the increase in the solid–vapor interface.* This equation can also predict the possibility of achieving superhydrophobic properties from intrinsically hydrophilic materials ( $\theta_Y < 90^\circ$ ) and even superoleophobic properties from intrinsically oleophilic materials ( $\theta_Y \text{ (oils)} < 90^\circ$ ).

## ❑ Effects of superhydrophobic surface pinned air layer

- In order for a surface to be superhydrophobic it must have a high contact angle ( $\theta \geq 150^\circ$ ). That generally means that water drops on the surface have, at least some, air between them and the surface (i.e., Cassie–Baxter regime).
- *A high quality superhydrophobic surface will have a uniform layer of pinned or trapped air that produces a very high contact angle (approaching  $180^\circ$ ), a very low roll-off angle (approaching  $0^\circ$ ), small contact angle hysteresis (approaching  $0^\circ$ ), and will produce an optical mirror effect when the surface is submerged in water due to total internal reflections of light reflecting off the pinned air layer.*
- Note that the pinned or trapped air in a high quality superhydrophobic surface acts as a physical barrier to liquid water or aqueous solutions but is not a barrier to the air, or gasses in general.
- *The utility of ultrahydrophobic surfaces extends to commercial applications of coatings and paints and many other applications.*

## Natural Superhydrophobic (SH) Surfaces

- There are many examples of naturally occurring superhydrophobic surfaces.
- These include both plants' and insects' surfaces.
- The *most notable natural superhydrophobic surface is that of the lotus leaf*. The extreme water repellency exhibited by lotus leaves is what *inspired scientists to initially pursue research into superhydrophobic phenomena*. In fact, the term '*lotus effect*' is still synonymous with *superhydrophobic behavior*. But *lotus effect* is little more than this that we shall see later.



(a)



(a)

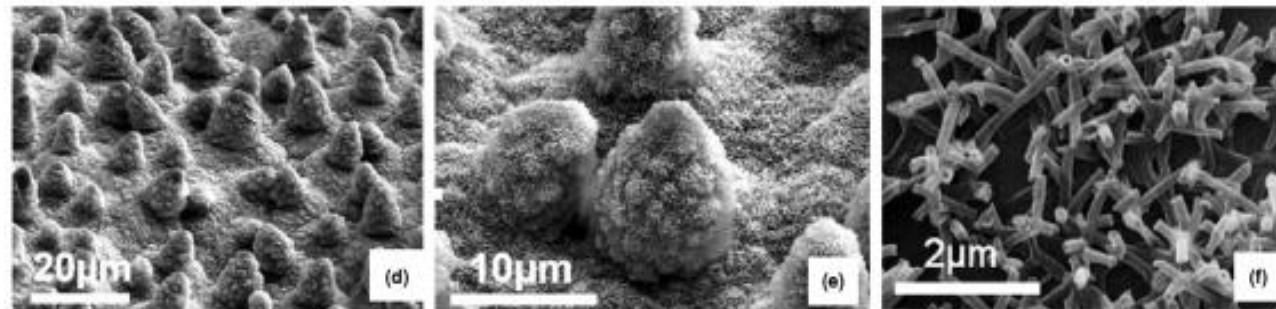
Fig. 3. (a) Lotus leaf: Water droplet beading on lotus leaf with *static contact angle* higher than 150 degrees.



➤ How is  $\theta_Y > 150^\circ$  achieved on lotus leaves?

We shall discuss it in the following sections.

- Scanning electron microscopy studies of the lotus leaf have shown that it has a surface **roughness** on **two length scales**.
- There are **pillars-like structures** on the surface called **micropapillae**, which are 0.5 to 20  $\mu\text{m}$  high three-dimensional wax crystals.
- However, Cheng and coworkers also reported that **the wax of the lotus leaves is hydrophilic** ( $\theta_Y = 74^\circ$ ).
- The surface of the micropapillae, in turn, is **nanostructured at a scale of about 120 nm** and the composition is various and includes long-chain hydrocarbons and derivatives with carbon chain lengths between 20 and 60 atoms.



**Figure 4.** Images of a superhydrophobic lotus leaves (*Nelumbo nucifera*) with self-cleaning properties at different magnifications. d, e & f: **Three different magnification of SEM images showing morphological micro- and nanostructures.**

- It is estimated that the structure of the lotus leaf reduces the ***fraction in contact*** to less than 0.01 or less than one percent.
- Lotus leaves (*Nelumbo nucifera*) are characterized by  $\theta_Y > 150^\circ$ , ultra-low water adhesion (ultra-low CA hysteresis and  $\alpha$ ) and self-cleaning properties.
- *Due to this superhydrophobicity, a water drop does not wet the surface and easily rolls off, taking with it any dirt on the surface, making the surface self-cleaning. This effect is called the “lotus effect”.*
- In fact, the mobility in a very highly hydrophobic surface can cause the drop to move across the surface and pick up small dirt particles, in effect causing a cleaning of the surface in the process. *This **self-cleaning effect** of a drop on a highly structured surface commonly referred to as the **lotus effect***, since it is observed on the leaf of the lotus flower (as well as on other leaves).
- The extreme water repellency exhibited by lotus leaves is what inspired scientists to initially pursue research into superhydrophobic phenomena. In fact, the term ‘lotus effect’ is still synonymous with superhydrophobic behavior.

## LOTUS EFFECT:

- The most famous example of natural superhydrophobic surfaces are lotus leaves (*Nelumbo nucifera*), which are characterized by  $\theta_Y > 150^\circ$ , ultra-low water adhesion and ***self-cleaning properties***.
- *Due to this superhydrophobicity, a water drop does not wet the surface and easily rolls off, taking with it any dirt on the surface, making the **surface self-cleaning**. This effect is called the “lotus effect”.*

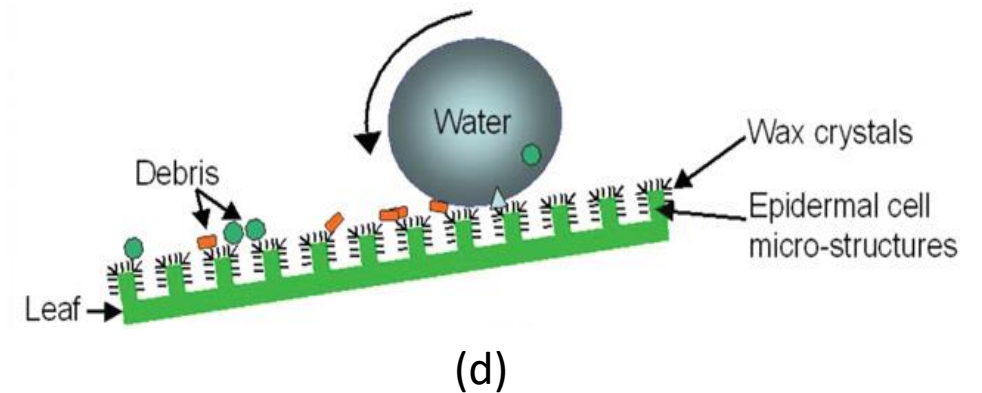
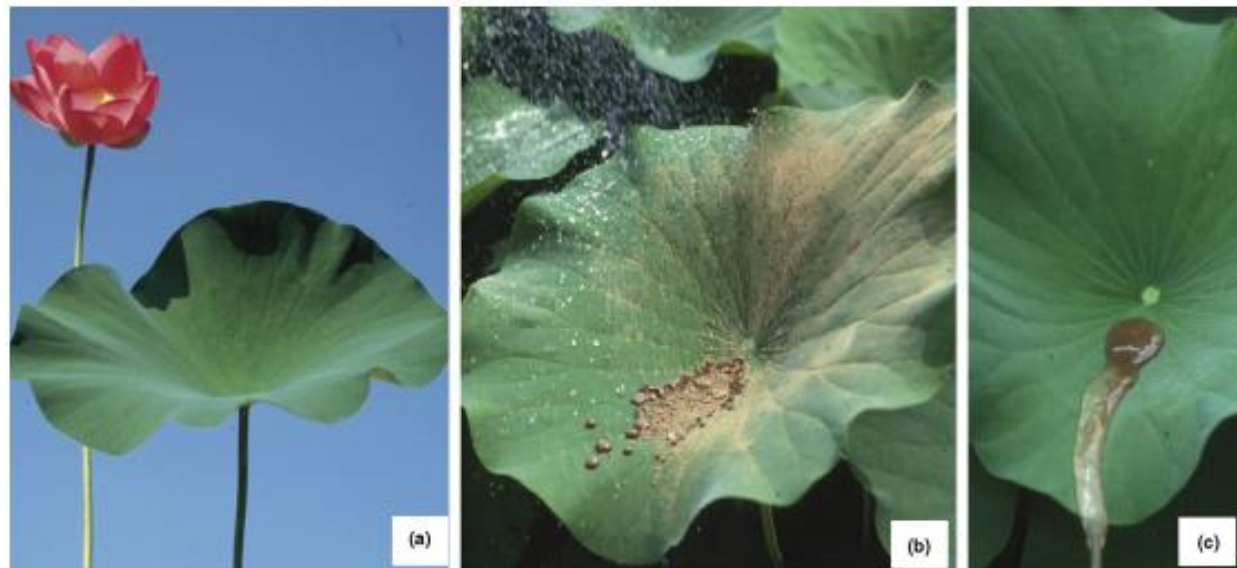


Fig. 3. (a-c) Lotus leaf: Water droplet beading on lotus leaf with *static contact angle* higher than 150 degrees.

(d) Schematic illustration of lotus effect.

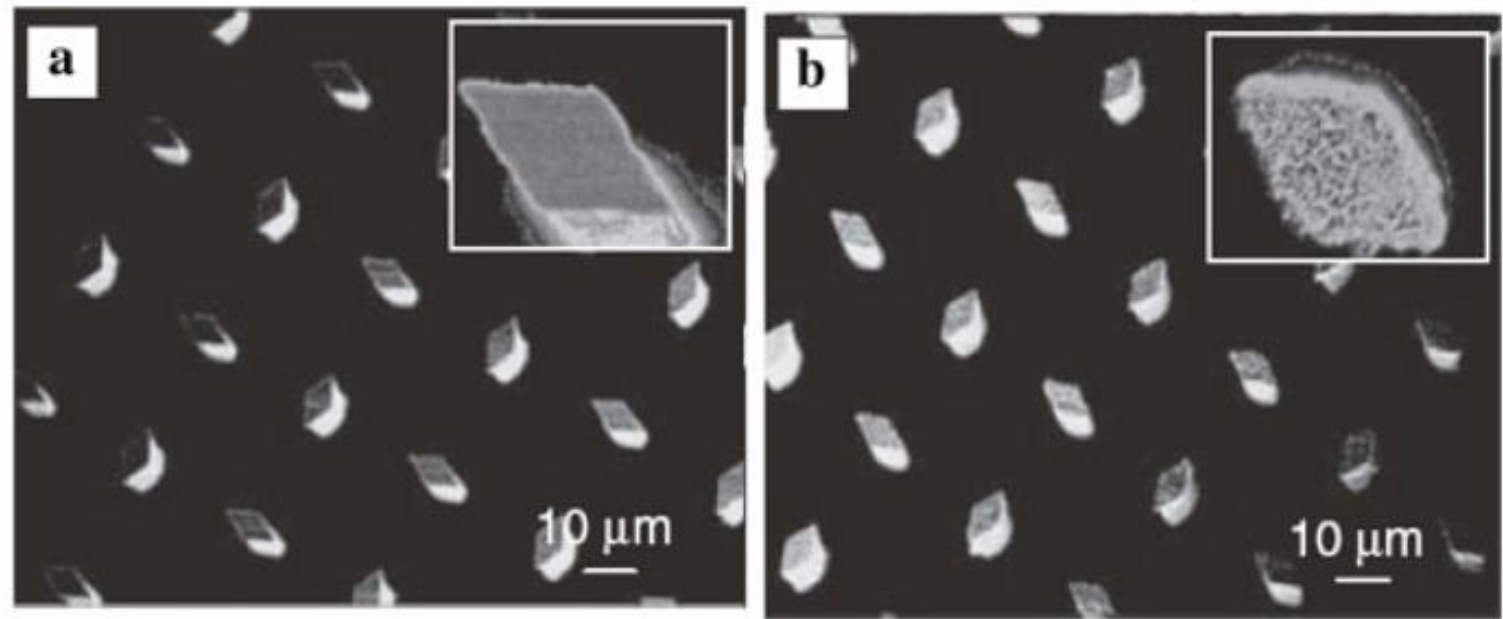
- Boreyko and Chen also confirmed the hydrophilicity of the lotus leaves by condensation experiments showing that the Wenzel state is the thermodynamically stable state on the lotus leaves and that the Cassie–Baxter state is metastable.
- *The self-cleaning properties (properties to remove dust and particles by the moving of water droplets)* are derived from the Cassie–Baxter state. This property is the consequence of a dual (micro/nano) surface structure. The duality is very important to stabilize the Cassie–Baxter state even after pressures corresponding to the impact of rainfall. At the microscale (Fig. 4d) the leaf contains convex cell papilla, while at the nanoscale (Fig. 4 e & f) epicuticular wax (lipid) crystals are observed. As the spherical water droplets roll around easily on the leaf, they encounter debris and other particulates which minimally adhere to the surface with multiple length scales of roughness and therefore can be readily carried away by the traversing water droplet. **This superhydrophobic effect is the origin of self-cleaning.** The self-cleaning effect is unavailable on a hydrophilic surface with non-spherical water droplets.
- Indeed, it is possible to achieve superhydrophobic properties from intrinsically hydrophilic materials as well as superoleophobic properties from intrinsically oleophilic materials.
- The *main requirement* was found to be *the presence of re-entrant structures*, also called **multivalued roughness topographies**, *which can strongly pin the liquid–vapor interface*. The air trapped below re-entrant structures can induce a negative Laplace pressure difference changing the liquid–vapor interface from concave to convex and impeding liquid penetration.



- ❖ In a *model artificial lotus leaf* (Fig. 11.64a, b) with **micrometer smooth posts**, water contact angles of  $\theta_{ad}/\theta_{rc} = 176^\circ/156^\circ$  are measured (Fig. 11.64a),
- ✓ whereas with **nanoscopic roughness** on the posts (Fig. 11.64b) nearly perfect hydrophobicity  $\theta_{ad}/\theta_{rc} \Rightarrow 176^\circ / > 176^\circ$  is found.
- ✓ From this, it is concluded that the *nano-hair* on the bumps of the lotus leaf ***substantially enhances hydrophobicity*** by ***increasing the local receding contact angle***.

Fig. 11.64 (a, b) Model artificial lotus leaves. (a) Scanning electron micrograph (SEM) of a surface containing micrometer-sized posts ***with a smooth surface***.

(b) Post from (a) covered *with nanosized methylsilicone fibrils* ( $\sim 40$  nm in diameter; see inset) yielding superhydrophobic properties.



## ❑ Applications of superhydrophobic surfaces and coatings

- Materials with superhydrophobic or superoleophobic properties are in extreme demand due to various potential applications such as in *anti-corrosion coatings, anti-icing coatings, liquid-repellent textiles, oil/water separation, nanoparticles assembly, microfluidic devices, printing techniques, optical devices, high-sensitive sensors or batteries*. In many of these applications, the presence of an air layer trapped inside the surface roughness can reduce the liquid penetration (oil/water separation, anti-fogging), the ion penetration (anti-corrosion, water desalination, batteries), the heat transfer (anti-icing), while the surface roughness can improve the intrinsic properties of the materials (optical, electrical, catalytic properties). It is also extremely important that the superhydrophobic coating is robust, which means the materials keep their properties even after high pressure.
- With the recent advances in durable superhydrophobic surfaces and coatings, there will soon be a large number of existing products converted into superhydrophobic products. The commercial introduction of durable superhydrophobic coatings, paints, and surfaces will have a dramatic worldwide effect on nearly every industry and possibly everyone on the earth.



### ➤ *Water repellency*

Water repellency is the most obvious application of superhydrophobic coatings and surfaces. The complete list of possible water repellency applications would be extensive and too long to include here. A partial list includes clothing that will be both *breathable and water repellant, umbrellas that stay completely dry, building materials, paints, epoxies, and silicones.*

### ➤ *Self-cleaning optical windows and lenses*

Optically clear superhydrophobic coatings on glasses, windows, and optical lenses will make seeing in foul weather much easier, and cleaning windows will be as simple as spraying them with water.

### ➤ *Viscous drag reduction*

Superhydrophobic paints and epoxies could greatly reduce the cost of transporting goods by ships and improve the efficiency of watercraft of all kinds due to the reduction of water drag on the watercraft's hull.

### ➤ *Anti-icing*

Superhydrophobic coatings and oil-modified superhydrophobic coatings could greatly reduce or even eliminate many of the effects of ice storms and aircraft icing.

### ➤ *Anti-corrosion*

Low permeability paint, used as a water and vapor barrier, is the standard way of protecting metal surfaces from corrosion. Such paint works well until the paint develops micro-cracks. At that point, water seeps into the micro-cracks. From then on, the paint, acting as a barrier, actually holds the water in the micro-cracks, which from that point on promotes corrosion. Volumetric superhydrophobic coatings prevent corrosion in an entirely different way. Volumetric superhydrophobic coatings are very porous with very high permeability. As such, one would believe that these paints would be terrible at preventing corrosion, but recent salt fog chamber testing has shown the opposite is actually true.

## ❖ *Desalination*

*Evaporative desalination was the first and is generally acknowledged to be the easiest way of converting seawater into freshwater.* But virtually all large-scale desalination done in the world uses the more complicated and expensive method of reverse osmosis desalination. *The reason why evaporative desalination has been abandoned has to do with the maintenance cost involved and corrosive effects of the salt residue generated by evaporation of saltwater.* Volumetric superhydrophobic coatings are saltwater-based corrosion resistant and can greatly reduce or prevent any salt residue buildup. Therefore, *it is possible that the use of volumetric superhydrophobic coatings could finally make large-scale evaporative desalination commercially viable.*

- ✓ As an example, Figure 32 (Left) shows salt residue on an aluminium pan after seawater was poured into the pan and allowed to evaporate. Note that the salt residue climbed up and over the pan and was well bonded to the pan after evaporation. Figure 32 (Right) shows another aluminium pan that was first coated with a superhydrophobic coating before adding seawater and letting it evaporate. After the salt evaporated, it was noticed that no salt residue climbed up the pan. In fact, none of the salt actually stuck to the pan but instead formed a big salt crystal, which was easily removed from the pan and discarded.

**Figure 32.** Left: evaporated seawater in aluminum plate. Right: evaporated seawater in superhydrophobic treated aluminum plate.

